eLife

Reviewed Preprint
v2 • February 13, 2025
Revised by authors

Reviewed Preprint
v1 • April 15, 2024

Cell Biology

Control of ciliary transcriptional programs during spermatogenesis by antagonistic transcription factors

Weihua Wang, Junqiao Xing, Xiqi Zhang, Hongni Liu, Xingyu Liu, Haochen Jiang, Cheng Xu, Xue Zhao, Zhangfeng Hu

Institute of Microalgae Synthetic Biology and Green Manufacturing, School of Life Sciences, Jianghan University, Wuhan, China • Hubei Engineering Research Center for Protection and Utilization of Special Biological Resources in the Hanjiang River Basin, School of Life Sciences, Jianghan University, Wuhan, China • NO.1 Middle School Affiliated to Central China Normal University, Wuhan, China • Hubei Key Laboratory of Environmental and Health Effects of Persistent Toxic Substances, Jianghan University, Wuhan, China

eLife Assessment

This **valuable** study presents data suggesting the critical roles of two ancient proteins, XAP5 and XAP5L, in regulating the transcriptional program of ciliogenesis during mouse spermatogenesis. The supporting data are **solid**, and this work will be of interest to biomedical researchers studying ciliogenesis and reproduction.

https://doi.org/10.7554/eLife.94754.2.sa3

Abstract

Existence of cilia in the last eukaryotic common ancestor (LECA) raises a fundamental question in biology: how the transcriptional regulation of ciliogenesis has evolved? One conceptual answer to this question is by an ancient transcription factor regulating ciliary gene expression in both unicellular and multicellular organisms, but examples of such transcription factors in eukaryotes are lacking. Previously, we showed that an ancient transcription factor XAP5 is required for flagellar assembly in *Chlamydomonas*. Here, we show that XAP5 and XAP5L are two conserved pairs of antagonistic transcription regulators that control ciliary transcriptional programs during spermatogenesis. Male mice lacking either XAP5 or XAP5L display infertility, as a result of meiotic prophase arrest and sperm flagella malformation, respectively. Mechanistically, XAP5 positively regulates the ciliary gene expression by activating the key regulators including FOXJ1 and RFX families during the early stage of spermatogenesis. In contrast, XAP5L negatively regulates the expression of ciliary genes via repressing these ciliary transcription factors during the spermiogenesis stage. Our results provide new insights into the mechanisms by which temporal and spatial transcription regulators are coordinated to control ciliary transcriptional programs during spermatogenesis.

Introduction

Cilia and flagella are evolutionarily conserved hair-like microtubule organelles that project from the surfaces of most eukaryotic cells(Derderian, Canales, & Reiter, 2023; Mitchell, 2017). They play essential roles in sensory reception, signal transduction and cell movement(Goetz & Anderson, 2010; Nachury & Mick, 2019; Singla & Reiter, 2006). The dysfunction of cilia in humans leads to an emerging class of genetic diseases called ciliopathies classified into first-order and second-order ciliopathies(Ishikawa & Marshall, 2011; Lovera & Lüders, 2021; Reiter & Leroux, 2017). First-order ciliopathies are caused by aberrations in ciliary proteins, and second-order ciliopathies occur due to defects in non-ciliary proteins, such as transcription factors, that are required for cilia formation and function(Reiter & Leroux, 2017).

Cilia are complex organelles and are dynamically regulated during development and the cell cycle(Eggenschwiler & Anderson, 2007; Kasahara & Inagaki, 2021; Santos & Reiter, 2008). The transcriptional regulation of ciliary genes must be precisely coordinated during ciliogenesis(Choksi, Lauter, Swoboda, & Roy, 2014; Collins, Ventrella, & Mitchell, 2021; Lewis & Stracker, 2021; Thomas et al., 2010). In metazoans, several transcription factors, including FOXJ1 and RFXs, have been shown to be involved in directing the expression of ciliary genes(Stubbs, Oishi, Izpisua Belmonte, & Kintner, 2008; Swoboda, Adler, & Thomas, 2000; X. Yu, Ng, Habacher, & Roy, 2008). These key ciliary transcription factors show dynamic expression patterns during development and differentiation(Stubbs et al., 2008; Swoboda et al., 2000; X. Yu et al., 2008). However, how these key transcriptional programs are spatially and temporally controlled by cell type-specific transcription factors and signaling pathways in order to activate specific target ciliary genes and generate diverse cilia is largely unknown.

Despite transcriptional regulation of ciliary genes is required for ciliogenesis in both unicellular and multicellular organisms, the underlying mechanism mediating ciliary gene expression may be fundamentally different, as the two major transcription factors, FOXJ1 and RFXs, are absent from many unicellular organisms(Chu, Baillie, & Chen, 2010; Li et al., 2018; Piasecki, Burghoorn, & Swoboda, 2010; Vij et al., 2012). Cilia and ciliary genes have been highly conserved throughout evolution, suggesting that the regulation of ciliary genes could be programmed by yet undiscovered transcriptional mechanisms, which possibly coevolved with multicellularity. Recently, an ancient transcription factor, XAP5, is found to regulate ciliary gene expression in a unicellular organism, *Chlamydomonas reinhardtii*(Li et al., 2018). XAP5 is highly conserved among different species and is widely expressed across tissues(Martin-Tryon & Harmer, 2008; Mazzarella, Pengue, Yoon, Jones, & Schlessinger, 1997). In vertebrates, *XAP5-like* (*XAP5L*) with an intronless open reading frame originated in Therians via retrotransposition of the ancestral *XAP5*, and it is highly expressed during spermatogenesis(Sedlacek et al., 1999; A. Zhang et al., 2011). However, whether XAP5 and XAP5L play essential roles in cilia development in multicellular organisms remains unknown.

Here, we show that XAP5/XAP5L are antagonistic transcription factors required for ciliary transcriptional programs during spermatogenesis. XAP5 is widely expressed in different tissues, while XAP5L is exclusively present in the testes. To explore the roles of XAP5/XAP5L in ciliogenesis, we generated a *XAP5L* knockout (KO) mouse line and found that *XAP5L* KO male mice are infertile due to the malformation of sperm flagella. Interestingly, male mice with the loss of XAP5 protein in germ cells also exhibited infertile, due to the arrest of spermatogenesis in the meiotic prophase stage. These data suggest that XAP5/XAP5L play crucial roles in sperm flagellar assembly in a spatiotemporal manner. Mechanistically, XAP5 positively modulates transcriptional rewiring of ciliary genes via activating the key regulators including FOXJ1 and RFXs during the early stage of spermatogenesis. Conversely, XAP5L negatively regulates the transcriptional

program controlling ciliogenesis by repressing these ciliary transcription factors during the spermiogenesis stage. Thus, ciliary transcriptional programs are spatially and temporally controlled by XAP5/XAP5L antagonistic transcription factors during spermatogenesis.

Results

XAP5 and XAP5L are indispensable for male fertility

To explore the potential functions of XAP5/XAP5L during ciliogenesis *in vivo*, we performed Western blot analysis to investigate the spatiotemporal expression of XAP5/XAP5L in various mouse tissues. We observed that XAP5 protein was widely expressed in diverse tissues and present at all stages of postnatal testes maturation, whereas XAP5L protein was mainly present in the testes and its level increased dramatically from postnatal day 21 (P21) and continued into adulthood (**Figures 1A**, B). Next, we identified the specific testicular cell types expressing XAP5/XAP5L using published single-cell RNA-seq data(Jung et al., 2019). XAP5 mRNA was found predominantly expressed in spermatogonia, while XAP5L mRNA was observed in pachytene spermatocytes, and remained until elongating spermatids (**Figure 1C**). Consistent with the mRNA localization patterns, immunofluorescence staining showed that XAP5 protein was mainly detected in the nuclei of spermatogonia, whereas XAP5L protein was present in the nuclei of pachytene spermatocytes and spermatids within the seminiferous tubules, and neither of XAP5 or XAP5L was detected in mature sperm (**Figure 1D** and Figure S1).

To investigate the physiological function of the uncharacterized XAP5/XAP5L protein, we attempted to generate global KO mice using the CRISPR-Cas9 system. We successfully established a *XAP5L* KO mouse line (Figures S2A-C) and found that while all *XAP5L* KO mice survived to adulthood and appeared indistinguishable from the wildtype (WT) mice, *XAP5L* KO males were sterile (**Figures 1E**, F). Notably, generating mosaic F0 founders with *XAP5* mutant allele proved challenging, and no F1 generation inherited the mutant alleles from the few F0 founders in over a year of breeding experiments, underscoring the critical roles of XAP5 in mouse development. Subsequently, we generated floxed-*XAP5* mice and crossed them with *Stra8-GFPCre* knockin mice(Lin et al., 2017) to produce *XAP5* germline-specific KO mice (*XAP5* cKO) (Figures S2D-F). Similar in appearance to controls ($XAP5^{fl/Y}$), all *XAP5* cKO males were also found to be sterile (**Figures 1G**, H). Collectively, these results suggest that XAP5/XAP5L play essential roles in spermatogenesis.

XAP5 and XAP5L function at different stages of spermatogenesis

To uncover the cause of male infertility, we conducted gross and histological analyses of the testes from WT and *XAP5L* KO mice. There were no differences in the gross appearance of testis or in the weight of mouse body and testis between WT and *XAP5L* KO mice (**Figure 2A**), but the number of sperm collected from cauda epididymis of *XAP5L* KO mice was significantly lower than that from WT mice (**Figure 2B**), and sperm motility was significantly reduced in KO mice (**Figure 2C** and Videos S1, 2). Histological analysis did not reveal any severe abnormity in the seminiferous epithelial cycle of XAP5L KO testes (**Figure 2D**). Further examination of the morphology and structure of cauda epididymal sperm in *XAP5L* KO mice revealed significantly higher rates of abnormal flagella (**Figures 2E-G**), indicating that XAP5L is crucial for flagellar assembly during spermiogenesis.

We also investigated the spermatogenic defects in the seminiferous tubules and epididymis of *XAP5* cKO male mice. Notably, the testes of *XAP5* cKO males were significantly smaller compared to WT controls at P16 and older (**Figure 3A**). Many seminiferous tubules in P16 and older *XAP5* cKO males were vacuolated due to the absence of spermatocytes and spermatids, as indicated by the lack of XY body formation and the absence of PNA signal, a marker of spermatids and sperm, in *XAP5* cKO germ cells (**Figures 3B-D**). As a consequence, no sperm were observed in the adult

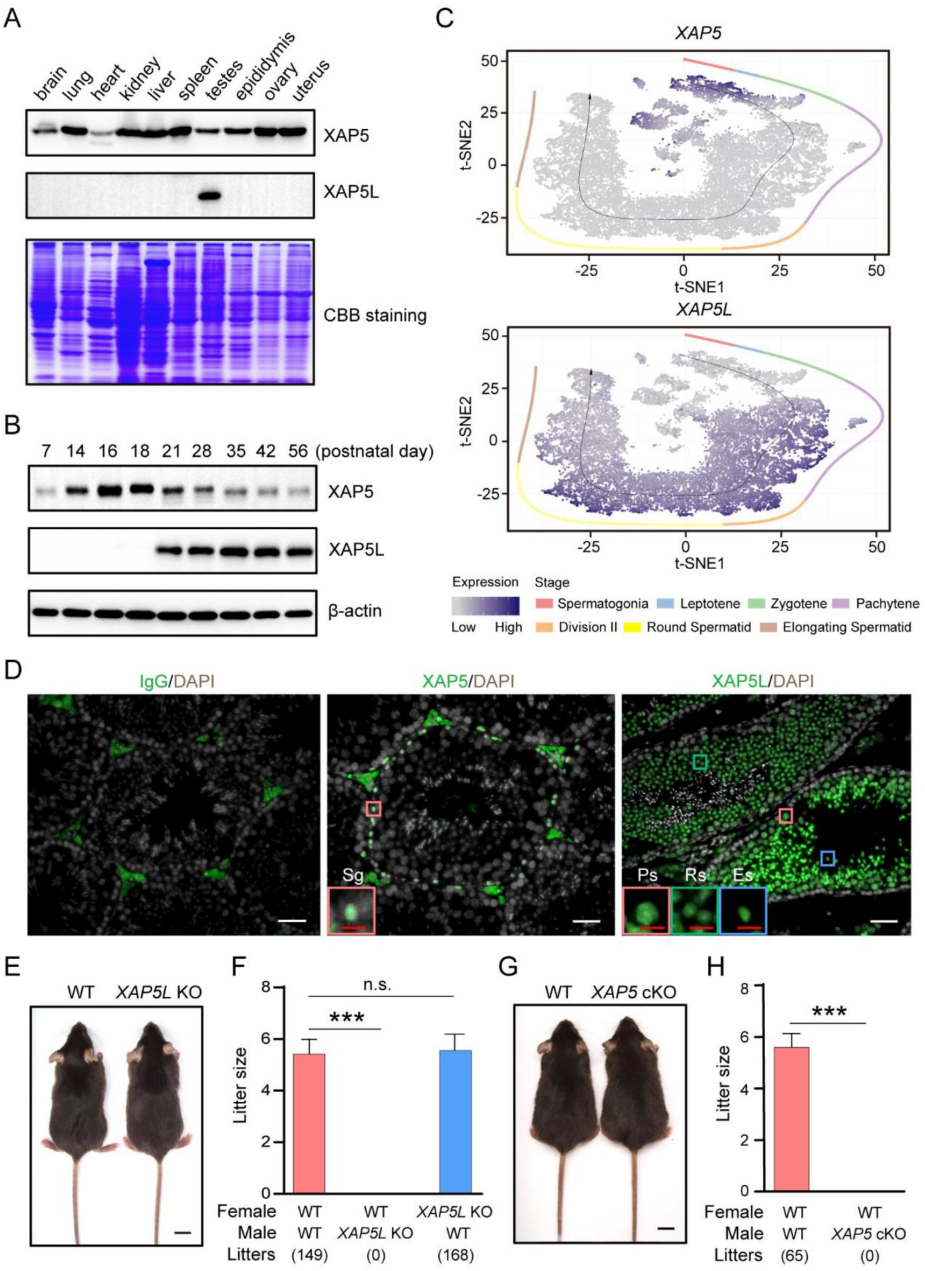

Figure 1.

Loss of XAP5 and XAP5L proteins results in male mice infertility.

(A) Detection of XAP5/XAP5L protein in different tissues of adult mice by Western blot analysis. **(B)** Expression of XAP5/XAP5L protein during postnatal testicular development. β-actin was used as control. **(C)** t-SNE plots displaying *XAP5*/*XAP5L* gene expression levels in individual cell types of mouse testis visualized using published single-cell data(Jung et al., 2019). Black arrow represents the developmental pseudotime corresponding to the developmental ordering of each cell progressing through spermatogenesis. Dot color intensity represents the expression level. Cells from different stages are color-coded. **(D)** Immunofluorescence staining of XAP5/XAP5L in adult WT testis. Representative spermatogonium (Sg), round spermatid (Rs) and elongating spermatid (Es) are indicated. Scale bars: 20 μm (white), 5 μm (red). **(E)** Similar development between WT and *XAP5L* KO mice. Scale bar: 1 cm. **(F)** Average litter size of pups obtained by fertility test. Each male was caged with two females for 2 months, 5 males were used for each genotype. ***$P < 0.001$, n.s. stands for not significant. **(G)** Similar appearance of WT and *XAP5* cKO mice. Scale bar: 1 cm. **(H)** Average litter size of pups obtained by fertility test. Each male was caged with two WT females for 2 months, 4 males were used for each genotype. ***$P < 0.001$. Error bars depict means ± SEM. All *P*-values were calculated using an unpaired, two-tailed Student's t-test.

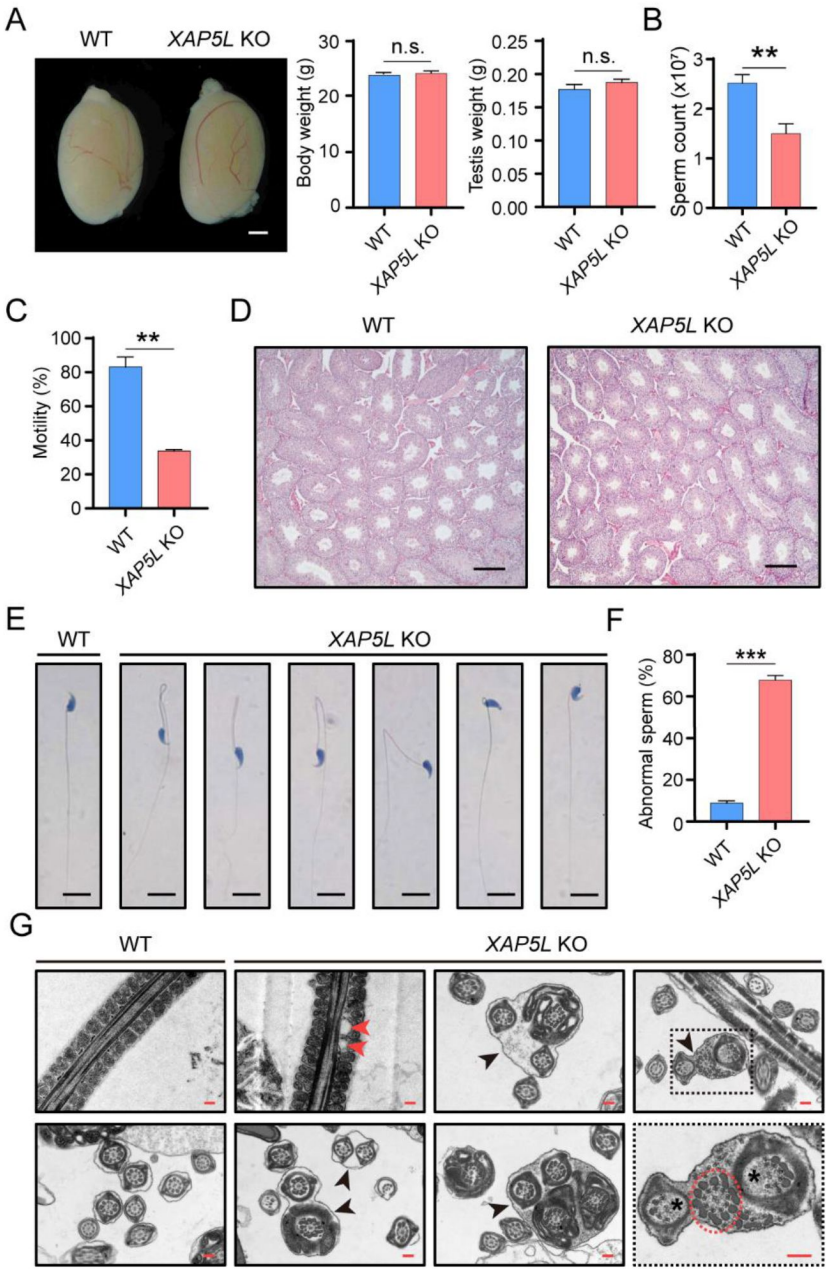

Figure 2.

XAP5L is required for normal sperm formation.

(A) Similar gross testes morphology, body weight and testis weight between WT and *XAP5L* KO mice. Scale bar: 1 mm. n = 6, n.s. stands for not significant. **(B)** Significantly reduced caudal epididymal sperm counts in XAP5L KO mice compared with WT males. n = 5, $^{**}P < 0.01$. **(C)** Significantly reduced sperm total motility of *XAP5L* KO mice. n =3, $^{**}P < 0.01$. **(D)** H&E staining showing similar histological structure of the testes from WT and *XAP5L* KO mice. Scale bars: 100 μm. **(E)** H&E staining showing the morphology of sperm in WT and *XAP5L* KO mice. Scale bars: 10 μm. **(F)** Significantly increased abnormal sperm in *XAP5L* KO mice. n = 6, $^{***}P < 0.001$. **(G)** Electron microscopic analysis displaying ultrastructural defects in *XAP5L* KO sperm flagella, including cytoplasmic vacuoles enveloping mitochondrial sheath (as shown by red arrowheads), a complete lack of mitochondrial sheath (as shown by red dotted circle), two or more cross-sections of the same sperm flagellum enclosed within one cell membrane (as shown by black arrowheads), partially formed outer dense fibers, and the axonemal microtubules (as indicated by asterisks). Scale bars: 2 μm. Error bars depict means ± SEM. All *P*-values were calculated using an unpaired, two-tailed Student's t- test.

cauda epididymides of *XAP5* cKO mice (**Figure 3E**). Taken together, these data indicate that germ cell development in *XAP5* cKO males was arrested in meiotic prophase, and XAP5 is indispensable for meiotic progression during spermatogenesis.

XAP5 and XAP5L function as antagonistic regulators of ciliary transcriptional regulatory networks via regulating transcription factors

To gain insight into the regulatory mechanisms of XAP5L during sperm flagellar assembly, we employed RNA-seq analysis to examine mature sperm collected from the cauda epididymis of WT and *XAP5L* KO adult mice. Differential expression analysis identified 2093 upregulated and 267 downregulated genes in *XAP5L* KO sperm (Figure S3A). Gene ontology analysis revealed that the upregulated genes were associated with cilia assembly or function (**Figure 4A** and Figures S3B, C). When crossed with the previously compiled ciliogenesis-related gene list(Nemajerova et al., 2016), the upregulated genes were observed encompassing diverse structural and functional components of the ciliogenic program (Table S1 and Figure S3D). Notably, several key transcription factor (TF) regulators of ciliogenesis were among the upregulated genes, including FOXJ1 and RFX families (**Figures 4B**, C and Figure S3E). Moreover, several key regulators of spermatogenesis, particularly spermiogenesis, were identified, including RFX2(Kistler et al., 2015; Wu et al., 2016), SOX families(Schartl et al., 2018; D. Zhang et al., 2018), TAF7L(Zhou et al., 2013) and TBPL1(Martianov et al., 2001) (**Figure 4B** and Figure S3E). Many core ciliary genes were also upregulated, such as *CFAP206*(Beckers et al., 2020) and *IFT81*(Qu et al., 2020) which are critical for male fertility (Figure S3E), consistent with the tight coregulation between spermiogenesis and cilia-related genes during spermatogenesis. These findings suggest that the genes identified in our study provide an excellent resource for candidates with novel ciliary or spermatogenesis-related functions, and the newly identified testes-specific protein TULP2(Oyama et al., 2022; Zheng et al., 2021) was selected for validation. We observed that *TULP2* KO male mice were sterile due to malformation of sperm flagella (Figure S4). Overall, our results clearly indicate that XAP5L acts as a central transcriptional repressor of ciliogenesis during mouse spermatogenesis.

Furthermore, we performed RNA-seq analysis using P16 testes samples from WT and *XAP5* cKO mice to explore the underlying mechanism of XAP5-mediated germ cell loss. Differential expression analysis identified 554 upregulated and 1587 downregulated genes in *XAP5* cKO sperm (Figure S5A). We observed that the downregulated genes in *XAP5* cKO males were involved in cilium assembly or functions (**Figure 4D** and Figures S5B-D). Strikingly, many of these downregulated genes were upregulated in *XAP5L* KO sperm, including the key ciliogenesis regulators FOXJ1 and RFX families (**Figures 4E**, F, Figure S5E and Table S1). In addition, meiosis initiation marker STRA8(Anderson et al., 2008; Ferder et al., 2019), meiosis-specific genes SPO11(Romanienko & Camerini- Otero, 2000) and DMC1(Bishop, Park, Xu, & Kleckner, 1992), key transcription regulators of spermiogenesis RFX2(Kistler et al., 2015; Wu et al., 2016), SOX30(D. Zhang et al., 2018) and CREM(Blendy, Kaestner, Weinbauer, Nieschlag, & Schutz, 1996; Nantel et al., 1996) were also downregulated in *XAP5* cKO mice (**Figures 4E** and S5F), consistent with the aforementioned result that loss of XAP5 induced spermatogenesis arrest in meiotic stage.

To identify direct targets of XAP5/XAP5L, we conducted CUT&Tag analyses on P16 mouse testicular germ cells for XAP5, and on P56 mouse testicular germ cells for XAP5L. Our results revealed 23143 peaks enriched for XAP5, compared to only 2290 peaks enriched for XAP5L (Table S1), and the limited number of enriched peaks for XAP5L suggests that the antibody used for XAP5L in the CUT&Tag experiment might have suboptimal performance. A substantial proportion of these peaks were located within promoter regions (Figures S6A, B), indicating that XAP5/XAP5L primarily function to regulate the expression of protein-coding genes. De novo motif analyses

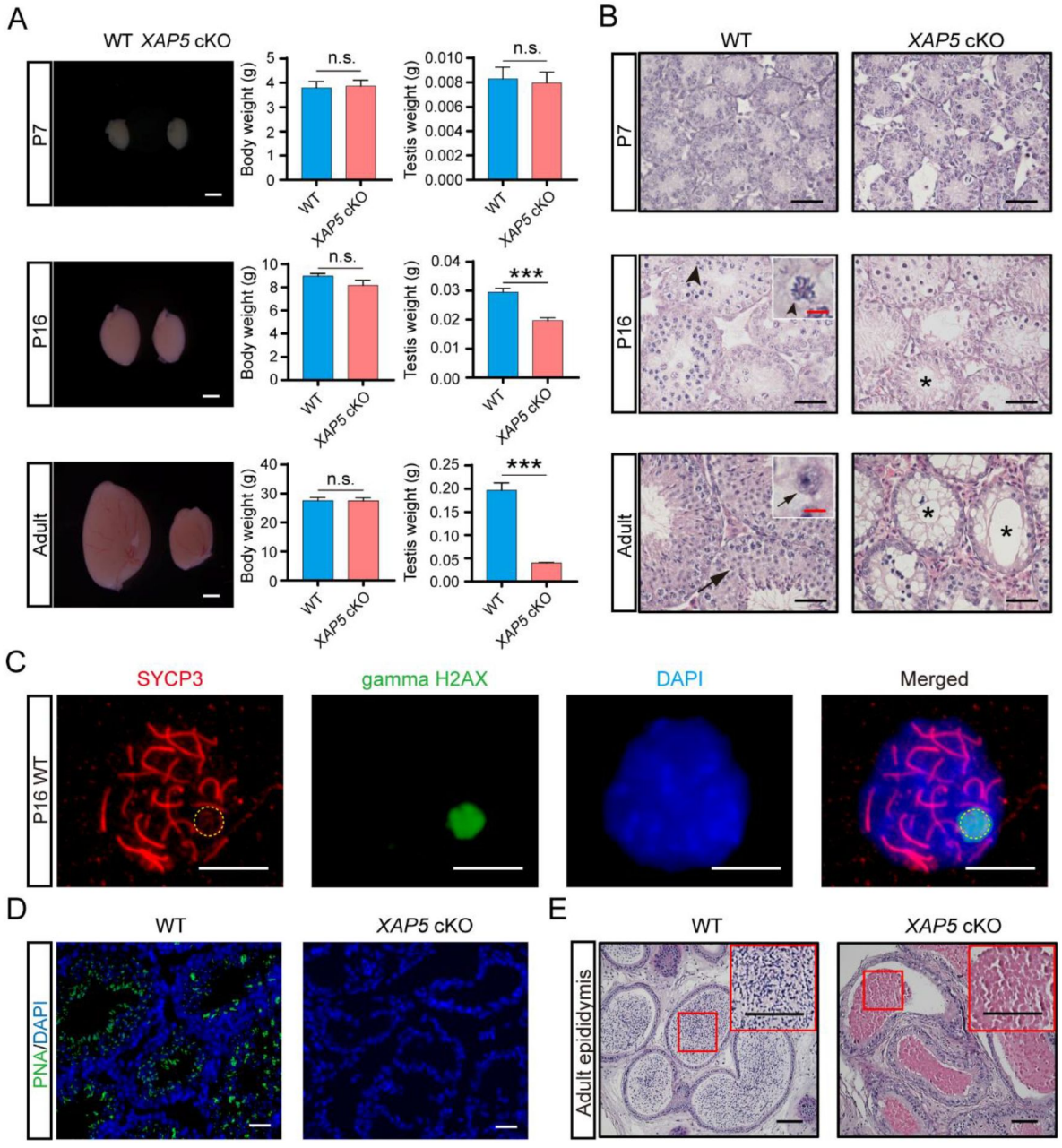

Figure 3.

Ablation of XAP5 in germ cells results in arrested spermatogenesis and absence of sperm.

(A) Testes sizes, body weight and testis weight from WT and *XAP5* cKO mice at various ages were evaluated. Similar body weight was observed between WT and *XAP5* cKO mice. No significant difference in size and weight was detected between WT and *XAP5* cKO testes until P16. Scale bars: 1 mm. n = 5, ***$P < 0.001$, n.s. stands for not significant. **(B)** Histology of testes from WT and *XAP5* cKO mice at various ages were evaluated by H&E staining. No pachytene spermatocytes were found, and many vacuolated tubules were observed in *XAP5* cKO testis since P16. Black arrowheads indicate pachytene spermatocytes; black arrows indicate round spermatids. Vacuolated seminiferous tubules are indicated by asterisks. Scale bars: 20 μm (black), 2.5 μm (red). **(C)** Chromosome spreads staining showing pachytene spermatocytes from P16 WT male mouse. Yellow dotted circle indicates the XY body. Scale bars: 10 μm. **(D)** Immunofluorescence staining of PNA in adult testes indicating the absence of spermatids in *XAP5* cKO mice. Scale bars: 20 μm. **(E)** H&E staining of adult epididymis displaying absence of sperm in *XAP5* cKO mice. Scale bars: 50 μm. Error bars depict means ± SEM. All *P*-values were calculated using an unpaired, two-tailed Student's t-test.

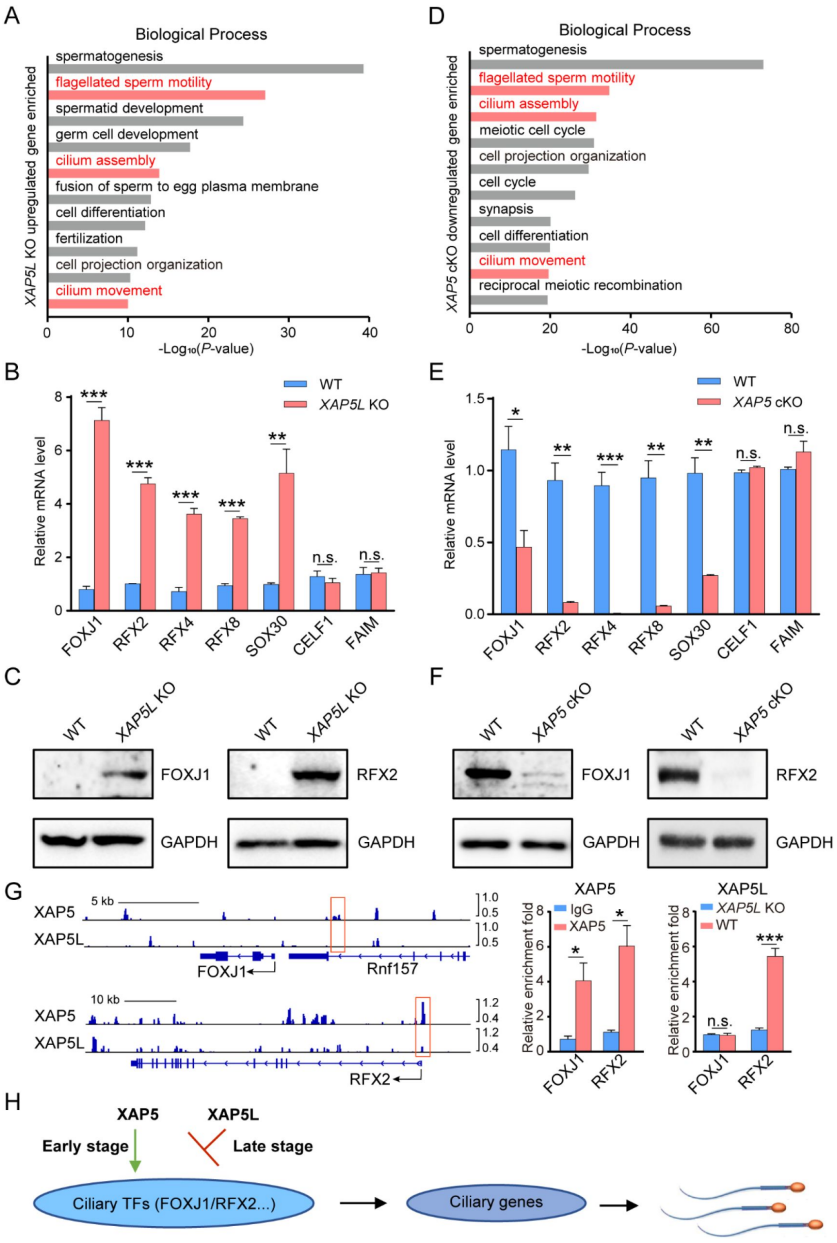

Figure 4.

Aberrant ciliogenic and spermatogenic gene expression in *XAP5L* KO and *XAP5* cKO male germ cells.

(A) Gene ontology analysis showing top ten biological process terms significantly enriched among upregulated genes in *XAP5L* KO sperm. **(B)** Real-time PCR validation of genes involved in ciliogenesis and spermatogenesis. n = 3, $^{**}P < 0.01$, $^{***}P < 0.001$, n.s. stands for not significant. **(C)** Detection of FOXJ1 and RFX2 in mature sperm of WT and *XAP5L* KO mice by Western blot analysis. GAPDH was used as a control. **(D)** Gene ontology analysis showing top ten biological process terms significantly enriched among downregulated genes in P16 *XAP5* cKO testes. **(E)** Real-time PCR validation of genes involved in ciliogenesis and spermatogenesis. n = 3, $^{*}P < 0.05$, $^{**}P < 0.01$, $^{***}P < 0.001$, n.s. stands for not significant. **(F)** Detection of FOXJ1 and RFX2 in P16 testes of WT and *XAP5* cKO mice by Western blot analysis. GAPDH was used as a control. **(G)** XAP5/XAP5L occupancies at *FOXJ1* and *RFX2* promoters assessed by CUT&Tag-seq (left) and CUT&Tag real-time PCR (middle and right). Red boxes indicate the binding regions of XAP5 and XAP5L. n = 3, $^{*}P < 0.05$, $^{***}P < 0.001$, n.s. stands for not significant. **(H)** A model on the involvement of XAP5 and XAP5L in the regulation of ciliogenesis during spermatogenesis. Error bars depict means ± SEM. All *P*-values were calculated using an unpaired, two-tailed Student's t-test.

showed that the binding motifs for XAP5 and XAP5L shared a conserved sequence (CCCCGCCC/GGGCGGGG) (Figure S6C), suggesting that XAP5 may regulate a subset of the same downstream genes as XAP5L.

To further elucidate the target genes of XAP5 and XAP5L, we integrated our CUT&Tag data with RNA-seq datasets (Table S1). This analysis revealed that among the genes downregulated in *XAP5* cKO germ cells, 891 were bound by XAP5 (Figure S6D). Similarly, 75 genes upregulated in *XAP5L* KO sperm were occupied by XAP5L (Figure S6E). GO analysis indicated that these genes are associated with cilium assembly and related functions (Figures S6D-G). Notably, both *FOXJ1* and *RFX2* are regulated and occupied by XAP5, with the conserved sequence present within the XAP5-bound regions (**Figure 4G**). Furthermore, real-time PCR validation of the CUT&Tag experiments confirmed that *RFX2* is also occupied by XAP5L, despite the initial CUT&Tag data not showing enriched peaks for the RFX2 gene (**Figure 4G**). Unfortunately, due to the suboptimal performance of the XAP5L antibody, we did not detect the occupancy of XAP5L on the FOXJ1 promoter. Nevertheless, these findings suggest that XAP5 and XAP5L regulate ciliary gene expression primarily through direct binding to the conserved motif present in these genes.

Considering the evolutionary conservation of XAP5/XAP5L protein across different species and the expression patterns of XAP5, XAP5L, FOXJ1 and RFX factors during spermatogenesis (**Figures 1C** and S7), these results suggest that XAP5 and XAP5L have antagonistic effects, and they may function upstream of the transcription factor families, including FOXJ1 and RFX factors, to coordinate the ciliogenesis during spermatogenesis (**Figure 4H**).

Discussion

Cilia and flagella are ancient organelles present in the last eukaryotic common ancestor (LECA) (Mitchell, 2017). Cilia assembly and maintenance are under strict transcriptional regulation in both unicellular and multicellular organisms(Choksi et al., 2014; Collins et al., 2021; Lewis & Stracker, 2021; Thomas et al., 2010). Despite cilia and flagella having an ancient origin, the evolutionary history of ciliary gene regulation has remained an unsolved problem. The main reason is that the master ciliary transcription factors found in multicellular organisms, including FOXJ1 and RFXs, are absent from unicellular organisms(Choksi et al., 2014; Collins et al., 2021; Lewis & Stracker, 2021; Thomas et al., 2010). Previously, we showed that an ancient transcription factor, XAP5, was required for flagella assembly in the unicellular green algae *Chlamydomonas*(Li et al., 2018). XAP5 proteins are evolutionarily conserved across diverse organisms(Li et al., 2018; Martin-Tryon & Harmer, 2008), which offers the possibility to investigate the conservation of the role of XAP5 in multicellular organisms. In the present study, we report that XAP5 positively regulates transcriptional network of ciliary genes by activating the key regulators including FOXJ1 and RFXs during spermatogenesis.

Cilia are dynamic organelles, and the expression profile of ciliary genes is dynamic during the cell cycle and under certain physiological conditions(Eggenschwiler & Anderson, 2007; Kasahara & Inagaki, 2021; Santos & Reiter, 2008). Cells have developed regulatory mechanisms to generate functional cilia in a temporal and spatial manner(Choksi et al., 2014; Collins et al., 2021; Lewis & Stracker, 2021; Thomas et al., 2010). However, how ciliary transcription factors determine temporal and spatial ciliary transcriptional programs is poorly understood. Sperm flagellar assembly is likewise tightly regulated during a highly complex temporal process named spermatogenesis(Holstein, Schulze, & Davidoff, 2003; Thomas et al., 2010). Several key transcriptional regulators of spermatogenesis, such as FOXJ1 and RFX2, have been identified(Chen, Knowles, Hebert, & Hackett, 1998; Kistler et al., 2015; Wu et al., 2016).

The flagellar formation of FOXJ1-null sperm is severely impaired, and the FOXJ1 target genes are required for sperm motility(Beckers et al., 2020; Chen et al., 1998; Weidemann et al., 2016). *RFX2* KO mice are completely sterile and RFX2 regulates the expression of ciliary genes during spermiogenesis(Kistler et al., 2015; Wu et al., 2016). Ciliary transcription factors (FOXJ1 and RFX2) are dynamically regulated during spermatogenesis(Jung et al., 2019). Intriguingly, our results show that XAP5 and XAP5L are two conserved pairs of antagonistic transcription factors that regulate these key transcriptional regulators required for spermatogenesis.

By using Western blot analysis, we found that XAP5 was ubiquitously expressed in all tissues examined, whereas XAP5L expression was restricted to the testes (**Figure 1A**). Interestingly, previous research found that XAP5L was widely expressed in normal tissue via using TCGA expression data(Thompson et al., 2021). Moreover, loss of XAP5/XAP5L perturbs transcriptional programs in cancer cells. At present, as shown by the recent data, we cannot rule out the possibility that XAP5L is dynamically expressed in other tissues during development. Although XAP5 and XAP5L are highly expressed in testes and critical for spermatogenesis, they are not present in mature sperm (Figure S1). Thus, XAP5/XAP5L are not needed for sperm maintenance. Given the dynamic expression of XAP5/XAP5L during spermatogenesis, it will be interesting to identify the key signaling factors that regulate the timely and spatial expression of XAP5 and XAP5L.

A role for XAP5 in human brain development is suggested by the association of X-linked intellectual disability (XLID) with rare *XAP5* missense variants(Lee et al., 2020).

However, how defects in XAP5 lead to XLID syndrome is unknown. Although there is as yet no evidence that XAP5 regulates ciliogenesis in any system besides *Chlamydomonas* and mice, the function in cilia could help clarify the unexplained role of *XAP5* mutations in causing XLID. The possibility that XAP5 could be a ciliary transcription factor in humans would add XLID to the growing list of the second-order ciliopathies.

Materials and Methods

Mice

C57BL/6J strains (from Vital River Laboratories, Beijing, China) and *Stra8-GFPCre* knockin mice (from Cyagen Biosciences) were used. Floxed-*XAP5* mice, *XAP5L* and *TULP2* knockout mice were generated on the C57BL/6J background using the CRISPR/Cas9 system. The sgRNA sequences used to target *XAP5*, *XAP5L* and *TULP2* were as follows: *XAP5L*, sgRNA1-GGC TAC CAG AAA CAG GGA CT, sgRNA2-GGG AGT AAG GTC CCC AAA CT; *XAP5*, sgRNA3-CTA CAG GGC ACT TAT TAA TA, sgRNA4-ATA GTA ATT CCC CCG TGC TT; *TULP2*, sgRNA5-TGA CTA ATT AGG CCC GAG AG, sgRNA6-GGT TCT TAG AGA GTC AAC GT. Experimental protocols were approved by the ethics committees of Jianghan University. Mice were maintained in a pathogen-free environment with a room temperature of 23 ± 2 °C under a humidity level of 30-70%. The light was maintained on a 12-hour day/night cycle.

Genome PCR

Mouse genomic DNA was isolated from the tail tip using One Step Mouse Genotyping Kit (Vazyme, PD101), and subjected to PCR with 2 × Taq Plus Master Mix (Vazyme, P212) following the manufacturer's instructions. The PCR products were separated by 2% agarose gel electrophoresis. The primers used are listed in Table S2.

RNA isolation and real-time PCR

Total RNA was isolated using the TRIzol reagent (Invitrogen, 15596018) and then converted to cDNA with HiScript II 1st Strand cDNA Synthesis Kit (Vazyme, R212) following the manufacturer's instructions. Real-time PCR was conducted using ChamQ SYBR qPCR Master Mix (Vazyme, Q311) on an ABI StepOnePlus real-time PCR system (Applied Biosystems). Expression values were normalized using the ΔΔCt method with *Gapdh* as the internal control. The primer sequences are indicated in Table S2.

Western blot analysis

Cell lysates from mouse tissues were prepared in RIPA buffer (Beyotime, P0013B) containing Protease Inhibitor Cocktail (Roche, 11873580001) and 1mM PMSF. Subcellular lysates of testicular nuclear and cytoplasmic fractions were prepared using Nuclear and Cytoplasmic Protein Extraction Kit (Beyotime, P0027) following the manufacturer's instructions. The protein lysates were subjected to standard immunoblotting analysis. Antibodies used were as follows: anti-β-actin (ABclonal, AC026), anti-XAP5 (Prospertech, HU-412003), anti-XAP5 (Sigma, HPA003585), anti-XAP5L (Prospertech, Hu-412001), anti-LMNB (Proteintech, 66095-1-Ig), anti-GAPDH (ABclonal, AC002), anti-FOXJ1 (D360355, Sangon Biotech), anti-RFX2 (K110716P, Solarbio) and anti-TULP2 (Prospertech, Hu-412002).

Immunofluorescence

Mouse testis were fixed in 4% paraformaldehyde in PBS at 4 °C overnight, dehydrated in gradient ethanol, embedded in paraffin, and sectioned into 5 μm slices. After deparaffinization and rehydration, testis sections were boiled in 1 mM EDTA, pH 8.0 for 15 min using a microwave oven for antigen retrieval, followed by cooling to room temperature. The primary antibodies, including anti-XAP5 (Prospertech, HU-412003, 1:250 dilution), anti-XAP5 (Sigma, HPA003585, 1:250 dilution), anti-XAP5L (Prospertech, Hu-412001, 1:250 dilution), anti-lectin PNA, Alexa Fluor 488 Conjugate (ThermoFisher, L21409, 1:250 dilution), and anti-TULP2 (Prospertech, Hu-412002, 1:250 dilution), were then incubated at 4 °C overnight. Subsequently, the sections were incubated with the secondary antibody donkey anti-rabbit Alexa Fluor Plus 488 (Invitrogen, A32790, 1:500 dilution) for 1 hour and DAPI for 5 minutes at room temperature. Images were collected using a Zeiss Axio Vert A1 microscope.

Histological analysis

Testes and epididymides were fixed in Bouin's solution (sigma, HT10132) overnight at 4 °C, embedded in paraffin and sectioned into 5 μm slices. The sections were then subjected to H&E staining using standard procedures and observed under a Zeiss Axio Vert A1 microscope.

Assessment of sperm counts, motility and morphology

Cauda epididymides were collected from male mice and dissected in 37°C pre-warmed human tubal fluid (HTF) culture medium (EasyCheck, M1130), followed by incubation at 37°C for 15 min to release the sperm. To quantify sperm abundance, the sperm suspension was fixed in 1% paraformaldehyde for 30 min. Sperm were then counted under a Zeiss ×10 bright-field microscope. To assess sperm motility, the sperm suspension was observed and recorded under a Leica total internal reflection fluorescence microscope. Motility was defined as any movement of the sperm flagellum during a 10- second observation cycle. After immobilization with 1% paraformaldehyde, sperm morphology was observed by H&E staining using standard procedures. Images were captured using a Zeiss Axio Vert A1 microscope equipped with a ×100 oil immersion objective. Sperm without staining were also used to assess sperm morphology. For ultrastructural observation, sperm samples were fixed in 3% glutaraldehyde in 0.1M sodium phosphate buffer (pH7.4), and post-fixed with 1% (wt/vol) OsO_4. After dehydration, the samples were placed in

propylene oxide and embedded in a mixture of Epon 812 and Araldite. Ultrathin sections obtained by a Leica EM UC7 ultramicrotome were stained with uranyl acetate and lead citrate, then analyzed using a HT7700 TEM (Hitachi).

Fertility test

Each of the adult male mice was mated with two females for 2 months. All the mice used were aged 6-8 weeks. Vaginal plugs were checked every morning, and the number of newborn pups was counted.

Chromosome spreads and immunofluorescence

Testicular chromosome spreads were prepared and immunolabeled as described(Reinholdt, Ashley, Schimenti, & Shima, 2004). The primary antibodies used were as follows: anti-γ H2AX (Millipore, 05-636, 1:300 dilution), anti-SYCP3 (Proteintech, 23024-1-AP, 1:300 dilution). Secondary antibodies used were Alexa Dye (AlexaFluor Plus 488/594) conjugates (ThermoFisher) at 1:500 dilutions. Images were collected with a Zeiss Axio Vert A1 microscope.

RNA-seq analysis

The mature sperm samples from P56 mice and testis samples from P16 mice were washed three time in 1× PBS after harvest. Total RNA was extracted from the samples using the TRIzol reagent (Invitrogen) and purified with the NEBNext Poly(A) mRNA Magnetic Isolation Module (NEB, E7490). The quality of the RNA samples was examined using the Agilent 2100 Bioanalyzer system (Agilent Technologies). Qualified RNA samples were subjected to sequencing library construction using the NEBNext Ultra II RNA Library Prep Kit for Illumina (NEB, E7775). Paired-end (2 × 150 bp) sequencing was carried out on the Illumina NovaSeq6000 platform. The sequencing reads were mapped to the Mus musculus reference genome (GRCm38/mm10) using HISAT2 v2.1.0(Kim, Langmead, & Salzberg, 2015), and StringTie v1.3.3b(Pertea et al., 2015) was applied to assemble the mapped reads. Fragments Per Kilobase of transcript per Million fragments mapped (FPKM) was used to measure the expression level of a gene. Differential expression analysis was processed by DESeq2 v1.12.4(Subramanian et al., 2005), and the significant differentially expressed genes were identified with a fold change >2. Gene Ontology analysis was performed using the DAVID database.

CUT&Tag analysis

The testicular germ cells were isolated using a two-step enzymatic digestion process as previously described (Liu et al., 2017). Briefly, after removing the tunica albuginea, the testes were incubated in 1 mg/mL type IV collagenase (Sigma, C5138) at 37°C for 15 min with gentle shaking every 5 min. The resulting cell suspension was centrifuged at 1000 rpm for 3 min, and the pellet was further digested with 0.25% Trypsin-EDTA (Gibco, 25200072) at 37°C for 10 min. The digestion was terminated by adding fetal bovine serum (FBS), and the cell suspension was centrifuged at 1000 rpm for 3 min. The cell pellet was resuspended in DMEM medium containing 10% FBS and cultured at 37°C in a 5% CO2 atmosphere for 3 h. Floating and weakly adherent cells were collected as germ cells. CUT&Tag and CUT&Tag real-time PCR were performed according to the manufacturer's protocol using the Hyperactive Universal CUT&Tag Assay Kit for Illumina Pro (Vazyme, TD904). Approximately 100,000 germ cells were used per sample. For real-time PCR, IgG sera were used as a negative control for the XAP5 CUT&Tag, while lysates from *XAP5L* KO testis were incubated with the XAP5L antibody as a negative control for the XAP5L CUT&Tag. DNA spike in was used as the internal control. The primer sequences are indicated in Table S2.

For analysis, quality control and read trimming were performed using FastQC (v0.11.9) with default parameters and Trimmomatic (v0.39) with the following parameters: ILLUMINACLIP:NexteraPE-PE.fa:2:30:10:8:true LEADING:3 TRAILING:3 SLIDINGWINDOW:4:15 MINLEN:8. Clean reads were aligned with bowtie2 (v2.4.4)(Langmead & Salzberg, 2012) against

the Mus musculus (mm39) genome with the parameters -X 1000 --very-sensitive. PCR duplicates were removed using picard's MarkDuplicates with default parameters. Peak calling was conducted using using MACS2 (v2.1.4) with the parameters -f BAMPE -B --SPMR --keep-dup all. Peaks were annotated to the nearest feature using ChIPseeker (v1.32.0)(G. Yu, Wang, & He, 2015). Motif finding and annotation were performed using Homer *findMotifsGenome.pl* and *annotatePeaks.pl* functions, respectively(Heinz et al., 2010). Track screen shots were produced in IGV (version 2.18.1)(Robinson, Thorvaldsdottir, Turner, & Mesirov, 2023).

Statistical analysis

Statistical analyses were conducted using GraphPad Prism 8.0.2 software. All data were presented as mean ± SEM. Values of $P < 0.05$ were considered statistically significant. Statistical significance between two groups was calculated using an unpaired, parametric, two-sided student's t test.

Materials and Data availability

The RNA-seq and CUT&Tag data generated in this study have been deposited in the Gene Expression Omnibus (GEO) database and are publicly available under accession numbers GSE236388 for RNA-seq and GSE279586 for CUT&Tag, respectively.

The authors declare that all the materials and the data supporting the findings of this study are available within the article and its supplementary materials or from the corresponding author upon reasonable request.

Supplementary figures

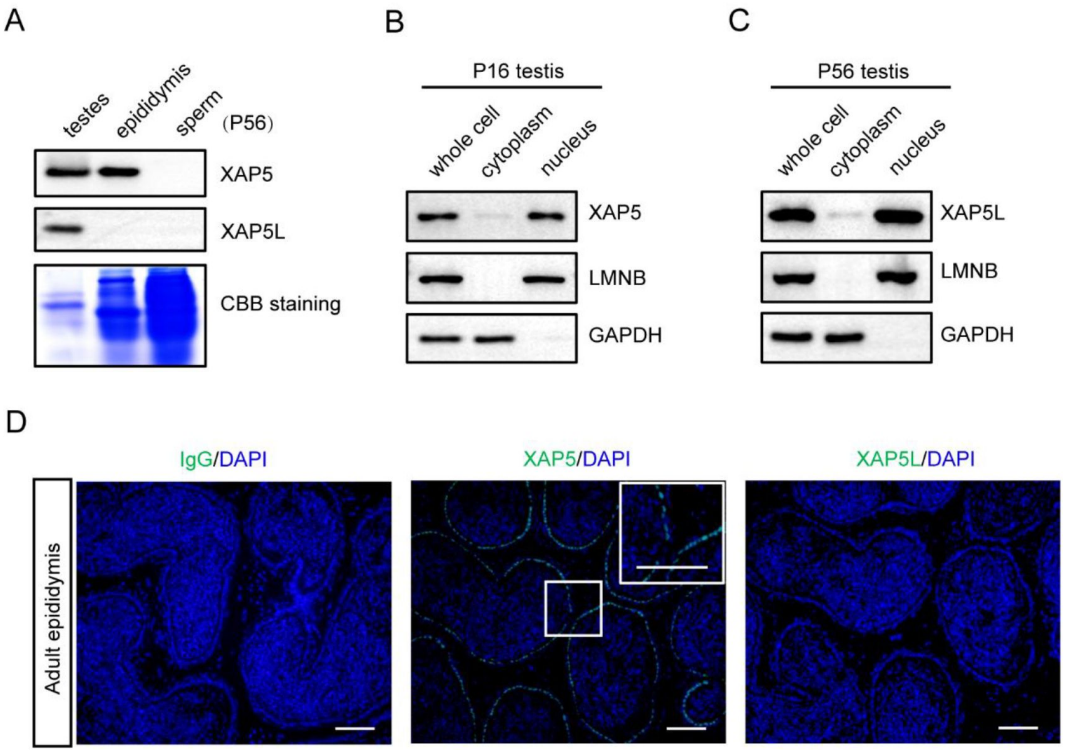

Figure S1.

Localization of XAP5/XAP5L in testicular cells.

(A) Western blot analysis showing no localization of XAP5/XAP5L in mature sperm. Western blot analysis showing the subcellular localization of endogenous XAP5 (**B**) and XAP5L (**C**). LMNB used as a nuclear protein marker, GAPDH used as a cytoplasmic protein marker. **(D)** Immunofluorescence staining of XAP5/XAP5L in adult epididymis. Scale bars: 50 μm.

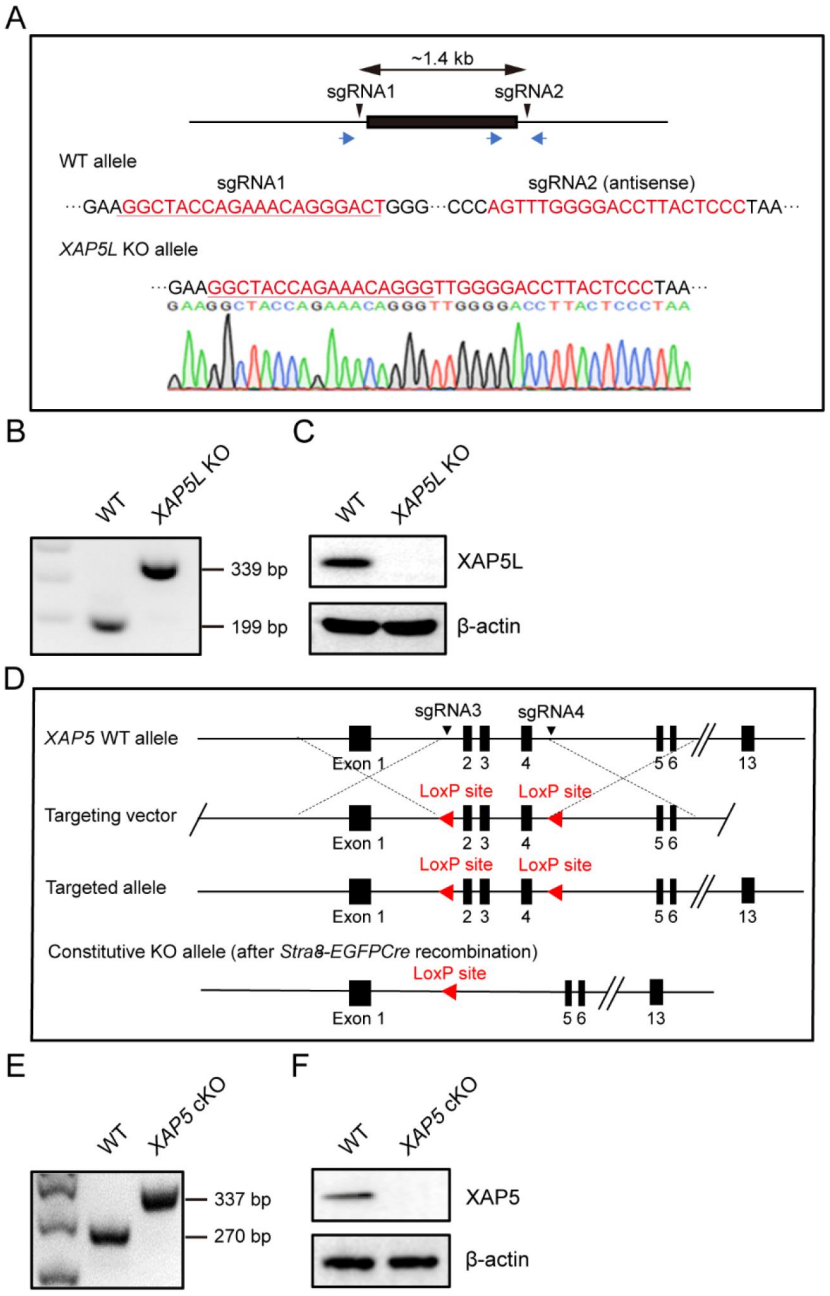

Figure S2.

Generation of *XAP5L* KO and *XAP5* cKO mice.

(A) Schematic illustration of the targeting strategy for generating a *XAP5L* knockout mouse line using CRISPR-Cas9 system. Upper panel showing genomic structure of the *XAP5L* gene. The location of two sgRNAs (sgRNA1 and sgRNA2) used and three primers (blue arrows) for genome PCR are indicated. Lower panel displaying nucleotide sequence of WT allele in the vicinity of two sgRNAs (red color) and the corresponding sequence of the *XAP5L* homozygous mutant (KO) allele. The deletion of *XAP5L* gene was verified by Sanger sequencing. **(B)** Genome PCR analysis in WT and *XAP5L* KO mice. **(C)** Detection of XAP5L in adult testes extracts of WT and *XAP5L* KO mice by Western blot analysis. β-actin was used as a control. **(D)** Schematic illustration of the targeting strategy for generating *XAP5* cKO mice. The location of LoxP sites inserted and the primers (blue arrow) used for genome PCR are indicated. **(E)** Genome PCR analysis in WT and *XAP5* cKO mice. **(F)** Detection of XAP5 in testes extracts of WT and *XAP5* cKO mice by Western blot analysis. β-actin was used as a control.

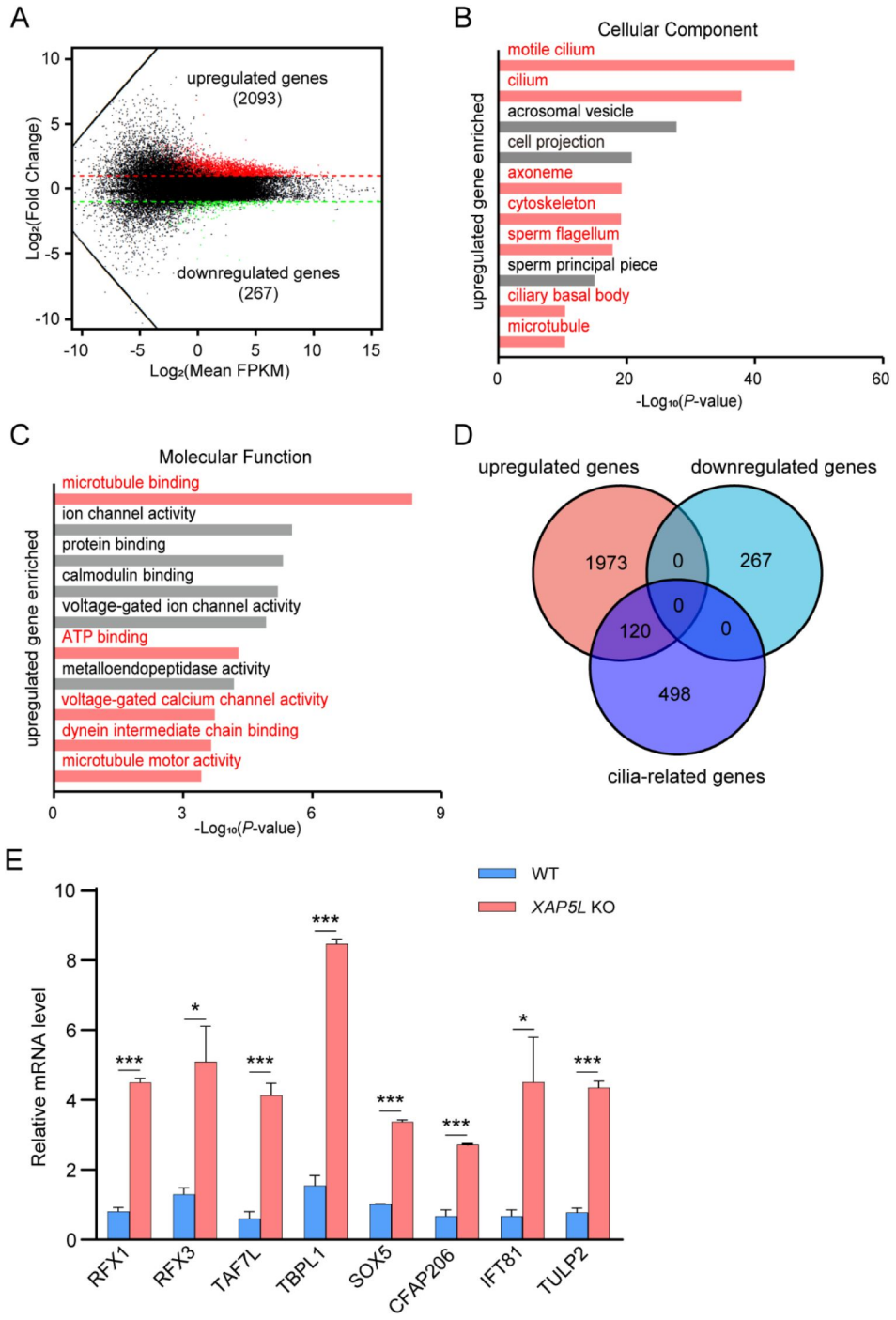

Figure S3.

XAP5L-mediated regulation of ciliary gene expression during mouse spermatogenesis.

(A) MA plot showing the numbers of differentially expressed genes in *XAP5L* KO sperm. Gene ontology analysis showing top ten cellular component (**B**) and molecular function (**C**) terms significantly enriched among upregulated genes in *XAP5L* KO sperm. **(D)** Venn diagram representing total genes upregulated/downregulated by at least twofold in *XAP5L* KO sperm and published cilia-related genes(Nemajerova et al., 2016). **(E)** Real- time PCR validation of genes involved in ciliogenesis and spermatogenesis. n = 3, **P* < 0.05, ****P* < 0.001. Error bars depict means ± SEM. All *P*-values were calculated using an unpaired, two-tailed Student's t-test.

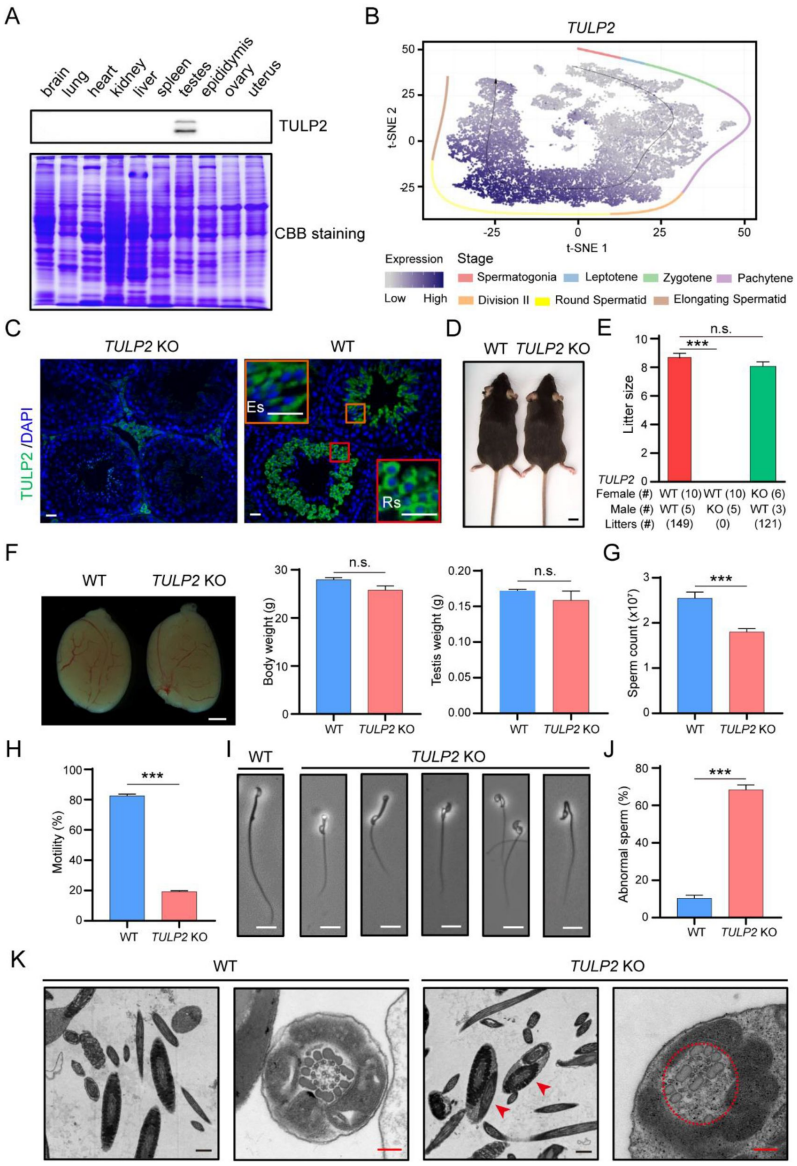

Figure S4.

TULP2 KO male mice were infertile due to malformation of sperm.

(A) Detection of TULP2 protein in different tissues of adult mice by Western blot analysis. **(B)** t-SNE plot displaying *TULP2* gene expression pattern during spermatogenesis visualized using published single-cell data(Jung et al., 2019). Black arrow represents the developmental pseudotime corresponding to the developmental ordering of each cell progressing through spermatogenesis. Dot color intensity represents the expression level. Cells from different stages are color-coded. **(C)** Immunofluorescence staining showing TULP2 expression in the cytoplasm of round spermatids (Rs) and elongating spermatids (Es). Scale bars: 5 μm. **(D)** Similar development of adult WT and *TULP2* KO mice. Scale bar: 1 cm. **(E)** Average litter size of pups obtained by fertility test. Each male was caged with two females for 2 months. ***$P < 0.001$, n.s. stands for not significant. **(F)** Similar gross testes morphology, body weight and testis weight between WT and *TULP2* KO mice. Scale bar: 1 mm. n = 4, n.s. stands for not significant. **(G)** Significantly reduced caudal epididymal sperm counts in *TULP2* KO mice compared with WT males. n = 7, ***$P < 0.001$. **(H)** Significantly reduced sperm total motility of *TULP2* KO mice. n = 3, ***$P < 0.001$. Significantly increased abnormal sperm in *TULP2* KO mice (**I** and **J**). Scale bars: 10 μm. n = 3, ***$P < 0.001$. **(K)** Electron microscopic analysis displaying ultrastructural defects in *TULP2* KO sperm flagella, including two cross-sections of the same sperm flagellum enclosed within one cell membrane (as shown by red arrowheads), disorganized outer dense fibers and the axonemal microtubules (as shown by red dotted circle). Scale bars: 8 μm (black), 2 μm (red). Error bars depict means ± SEM. All *P*-values were calculated using an unpaired, two-tailed Student's t-test.

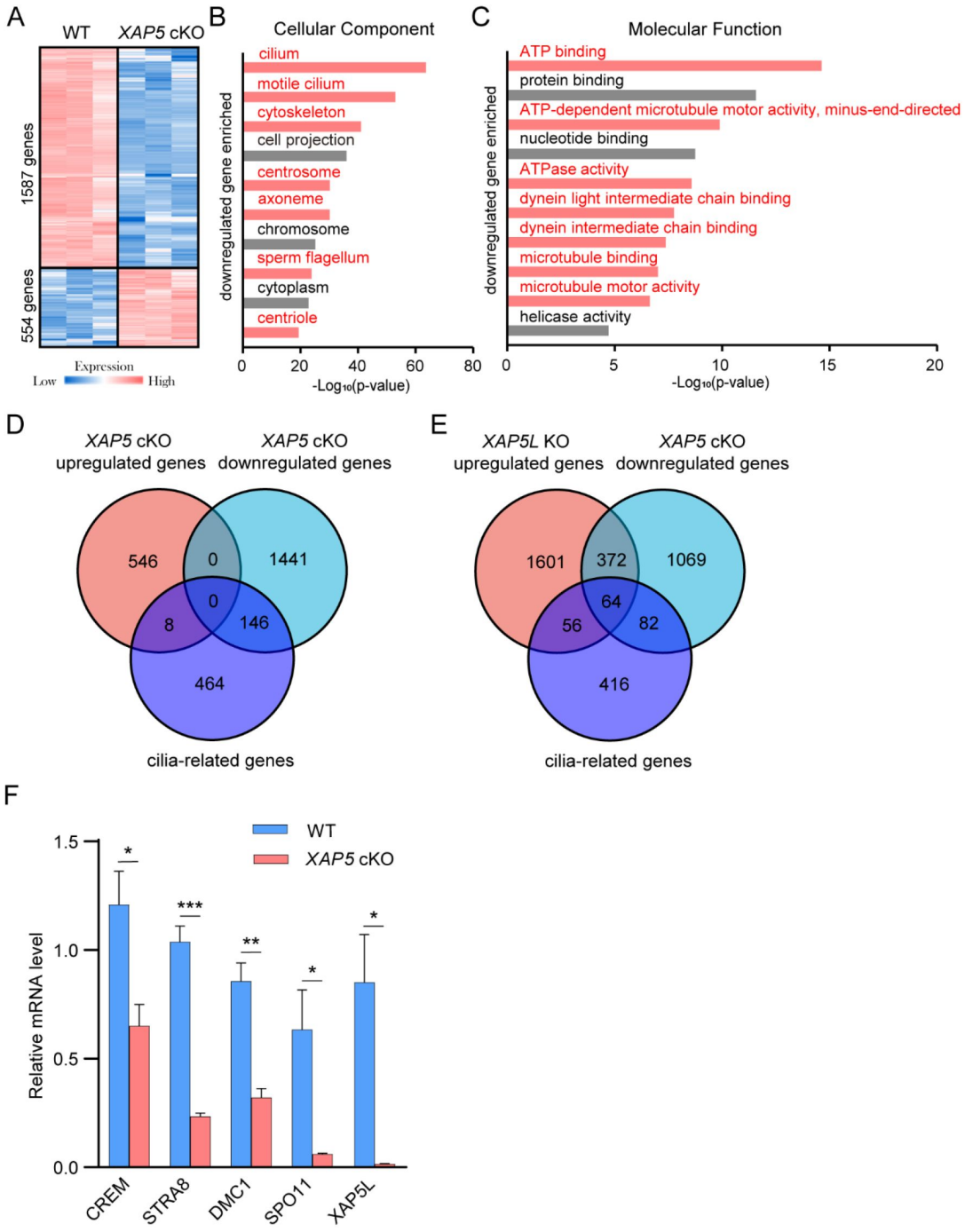

Figure S5.

XAP5-mediated regulation of ciliary gene expression during mouse spermatogenesis.

(A) Heat map showing variably expressed genes in P16 *XAP5* cKO testes. Number of related genes was indicated. Gene ontology analysis showing top ten cellular component and molecular function (**C**) terms significantly enriched among downregulated genes in *XAP5* cKO testes. **(D)** Venn diagram representing total genes upregulated/downregulated in *XAP5* cKO testes and published cilia-related genes(Nemajerova et al., 2016). **(E)** Venn diagram representing total genes downregulated in *XAP5* cKO testes, upregulated in *XAP5L* KO sperm by at least twofold and published cilia-related genes(Nemajerova et al., 2016). **(F)** Real-time PCR validation of genes involved in ciliogenesis and spermatogenesis. n = 3, **P* < 0.05, ***P* < 0.01, ****P* 0.001. Error bars depict means ± SEM. All *P*-values were calculated using an unpaired, two-tailed Student's t-test.

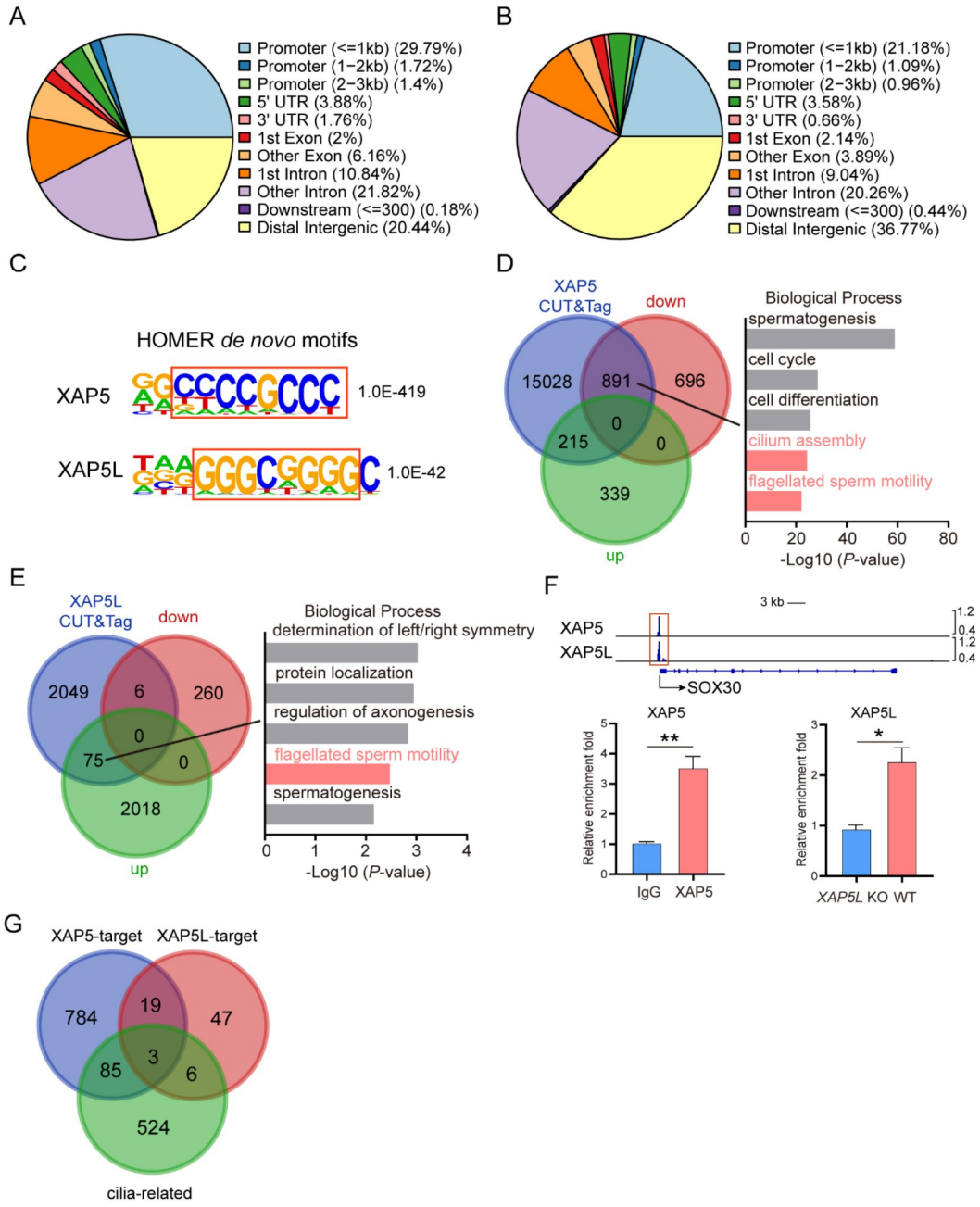

Figure S6.

Identification of XAP5/XAP5L-occupancy sites.

Location of XAP5 **(A)** and XAP5L **(B)**-occupancy peaks relative to the nearest annotated gene. **(C)** DNA sequence identified by Homer de novo motif analysis from XAP5/XAP5L peaks. The P value of the motif comparison is indicated. Overlapped sequences are shown in red boxes. (**D**) Left, overlapping genes identified by XAP5 CUT&Tag and RNA-seq analyses. Right, representative biological processes enriched among the overlapping genes that are downregulated in *XAP5* cKO germ cells and bound by XAP5 (as identified by CUT&Tag). (**E**) Left, overlapping genes identified by XAP5L CUT&Tag and RNA-seq analyses. Right, representative biological processes enriched among the overlapping genes that are upregulated in *XAP5* KO sperm and bound by XAP5L (as identified by CUT&Tag). (**F**) XAP5/XAP5L occupancies at *SOX30* promoter assessed by CUT&Tag-seq (top) and CUT&Tag real-time PCR (bottom). Red boxes indicate the binding regions of XAP5/XAP5L. n = 3, **P* < 0.05, ***P* < 0.01. (**G**) Overlapping genes among XAP5/XAP5L target genes (the 891 genes in Figure S6D and the 75 genes in Figure S6E) and published cilia-related genes(Nemajerova et al., 2016). Error bars depict means ± SEM. All *P*-values were calculated using an unpaired, two- tailed Student's t-test.

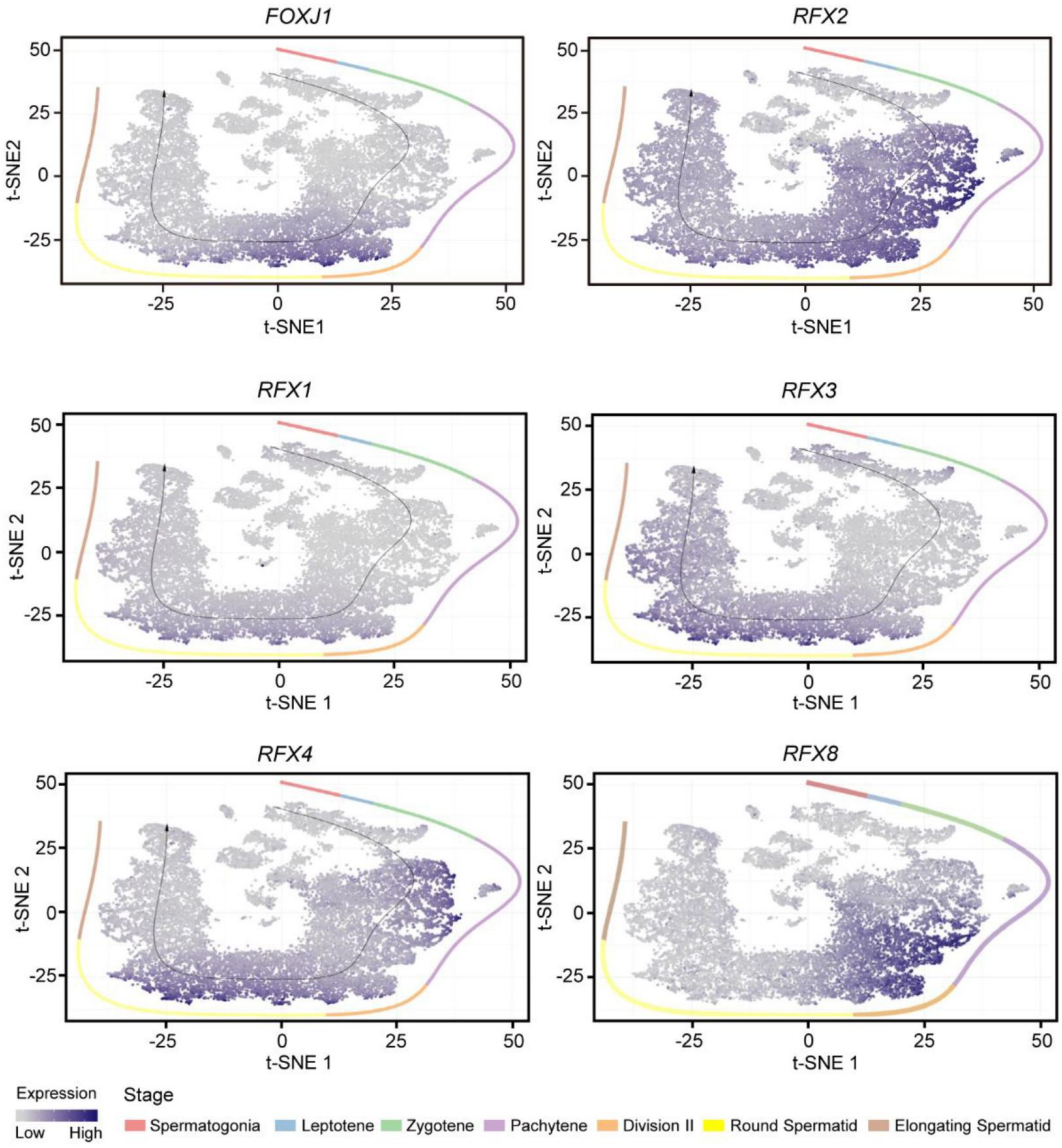

Figure S7.

t-SNE plots displaying expression patterns of *FOXJ1* and *RFX* families in individual cell types of mouse testes.

The black arrow represents the developmental pseudotime corresponding to the developmental ordering of each cell progressing through spermatogenesis. Dot color intensity represents the relative expression level. Cells from different stages are color- coded. The gene expression was visualized using the published single-cell data(Jung et al., 2019).

Acknowledgements

This work was supported by the National Key R&D Program of China (grant number: 2020YFA0907400), the National Natural Science Foundation of China (grant number: 32170702 and 82000828) and the Major Special Funding Program for First-class Discipline Construction of Jianghan University (grant number: 2023XKZ021). We thank

Yuan He (Research Center for Medicine and Structural Biology, Wuhan University, China) for the assistance during the experimental design of the transmission electron microscope analysis.

Additional information

Author Contributions

W.W., J.X., X.Z. and Z.H. designed research; W.W., J.X., X.Z., H.L., X.L., H.J., C.X. and X.Z. performed research; W.W. and Z.H. contributed new reagents/analytic tools; W.W., J.X., X.Z. and Z.H. analyzed data; and W.W. and Z.H. wrote the paper.

Additional files

Video S1. *Representative video of living sperm cells from WT mouse.*

Video S2. *Representative video of living sperm cells from XAP5L KO mouse.*

Table S1. *The lists of differential expression genes, ciliogenesis-related genes, and enriched peaks for XAP5/XAP5L.*

Table S2. *The lists of primers used in the Genome PCR and real-time PCR.*

References

1. Anderson E. L., Baltus A. E., Roepers-Gajadien H. L., Hassold T. J., de Rooij D. G., van Pelt A. M., Page D. C. 2008) **Stra8 and its inducer, retinoic acid, regulate meiotic initiation in both spermatogenesis and oogenesis in mice** *Proc Natl Acad Sci U S A* **105**:14976–14980 https://doi.org/10.1073/pnas.0807297105

2. Beckers A., Adis C., Schuster-Gossler K., Tveriakhina L., Ott T., Fuhl F., ..., Gossler A. 2020) **The FOXJ1 target Cfap206 is required for sperm motility, mucociliary clearance of the airways and brain development** *Development* https://doi.org/10.1242/dev.188052

3. Bishop D. K., Park D., Xu L., Kleckner N 1992) **DMC1: a meiosis-specific yeast homolog of E. coli recA required for recombination, synaptonemal complex formation, and cell cycle progression** *Cell* **69**:439–456 https://doi.org/10.1016/0092-8674(92)90446-j

4. Blendy J. A., Kaestner K. H., Weinbauer G. F., Nieschlag E., Schutz G 1996) **Severe impairment of spermatogenesis in mice lacking the CREM gene** *Nature* **380**:162–165 https://doi.org/10.1038/380162a0

5. Chen J., Knowles H. J., Hebert J. L., Hackett B. P 1998) **Mutation of the mouse hepatocyte nuclear factor/forkhead homologue 4 gene results in an absence of cilia and random left-right asymmetry** *J Clin Invest* **102**:1077–1082 https://doi.org/10.1172/JCI4786

6. Choksi S. P., Lauter G., Swoboda P., Roy S 2014) **Switching on cilia: transcriptional networks regulating ciliogenesis** *Development* **141**:1427–1441 https://doi.org/10.1242/dev.074666

7. Chu J. S., Baillie D. L., Chen N 2010) **Convergent evolution of RFX transcription factors and ciliary genes predated the origin of metazoans** *BMC Evol Biol* **10** https://doi.org/10.1186/1471-2148-10-130

8. Collins C., Ventrella R., Mitchell B. J 2021) **Building a ciliated epithelium: Transcriptional regulation and radial intercalation of multiciliated cells** *Curr Top Dev Biol* **145**:3–39 https://doi.org/10.1016/bs.ctdb.2020.08.001

9. Derderian C., Canales G. I., Reiter J. F 2023) **Seriously cilia: A tiny organelle illuminates evolution, disease, and intercellular communication** *Dev Cell* **58**:1333–1349 https://doi.org/10.1016/j.devcel.2023.06.013

10. Eggenschwiler J. T., Anderson K. V 2007) **Cilia and developmental signaling** *Annu Rev Cell Dev Biol* **23**:345–373 https://doi.org/10.1146/annurev.cellbio.23.090506.123249

11. Ferder I. C., Fung L., Ohguchi Y., Zhang X., Lassen K. G., Capen D., ..., Wang N. 2019) **Meiotic gatekeeper STRA8 suppresses autophagy by repressing Nr1d1 expression during spermatogenesis in mice** *PLoS Genet* **15** https://doi.org/10.1371/journal.pgen.1008084

12. Goetz S. C., Anderson K. V 2010) **The primary cilium: a signalling centre during vertebrate development** *Nat Rev Genet* **11**:331–344 https://doi.org/10.1038/nrg2774

13. Heinz S., Benner C., Spann N., Bertolino E., Lin Y. C., Laslo P., ..., Glass C., K 2010) **Simple combinations of lineage-determining transcription factors prime cis-regulatory elements**

required for macrophage and B cell identities *Mol Cell* **38**:576–589 https://doi.org/10.1016/j.molcel.2010.05.004

14. Holstein A.-F., Schulze W., Davidoff M 2003) **Understanding spermatogenesis is a prerequisite for treatment** *Reproductive Biology and Endocrinology* **1** https://doi.org/10.1186/1477-7827-1-107

15. Ishikawa H., Marshall W. F. 2011) **Ciliogenesis: building the cell's antenna.** *Nat Rev Mol Cell Biol* **12**:222–234 https://doi.org/10.1038/nrm3085

16. Jung M., Wells D., Rusch J., Ahmad S., Marchini J., Myers S. R., Conrad D. F 2019) **Unified single-cell analysis of testis gene regulation and pathology in five mouse strains** *Elife* **8** https://doi.org/10.7554/eLife.43966

17. Kasahara K., Inagaki M 2021) **Primary ciliary signaling: links with the cell cycle** *Trends Cell Biol* **31**:954–964 https://doi.org/10.1016/j.tcb.2021.07.009

18. Kim D., Langmead B., Salzberg S. L 2015) **HISAT: a fast spliced aligner with low memory requirements** *Nat Methods* **12**:357–360 https://doi.org/10.1038/nmeth.3317

19. Kistler W. S., Baas D., Lemeille S., Paschaki M., Seguin-Estevez Q., Barras E., ..., Reith W. 2015) **RFX2 Is a Major Transcriptional Regulator of Spermiogenesis** *PLoS Genet* **11** https://doi.org/10.1371/journal.pgen.1005368

20. Langmead B., Salzberg S. L 2012) **Fast gapped-read alignment with Bowtie 2** *Nat Methods* **9**:357–359 https://doi.org/10.1038/nmeth.1923

21. Lee Y.-R., Khan K., Armfield-Uhas K., Srikanth S., Thompson N. A., Pardo M., ..., Schwartz C. E. 2020) **Mutations in FAM50A suggest that Armfield XLID syndrome is a spliceosomopathy** *Nature Communications* **11** https://doi.org/10.1038/s41467-020-17452-6

22. Lewis M., Stracker T. H 2021) **Transcriptional regulation of multiciliated cell differentiation** *Semin Cell Dev Biol* **110**:51–60 https://doi.org/10.1016/j.semcdb.2020.04.007

23. Li L., Tian G., Peng H., Meng D., Wang L., Hu X., ..., Hu Z. 2018) **New class of transcription factors controls flagellar assembly by recruiting RNA polymerase II in Chlamydomonas** *Proc Natl Acad Sci U S A* **115**:4435–4440 https://doi.org/10.1073/pnas.1719206115

24. Lin Z., Hsu P. J., Xing X., Fang J., Lu Z., Zou Q., ..., Tong M. H. 2017) **Mettl3-/Mettl14-mediated mRNA N(6)-methyladenosine modulates murine spermatogenesis** *Cell Res* **27**:1216–1230 https://doi.org/10.1038/cr.2017.117

25. Liu W., Wang F., Xu Q., Shi J., Zhang X., Lu X., ..., Li L. 2017) **BCAS2 is involved in alternative mRNA splicing in spermatogonia and the transition to meiosis** *Nat Commun* **8** https://doi.org/10.1038/ncomms14182

26. Lovera M., Lüders J 2021) **The ciliary impact of nonciliary gene mutations** *Trends Cell Biol* **31**:876–887 https://doi.org/10.1016/j.tcb.2021.06.001

27. Martianov I., Fimia G. M., Dierich A., Parvinen M., Sassone-Corsi P., Davidson I 2001) **Late arrest of spermiogenesis and germ cell apoptosis in mice lacking the TBP-like TLF/TRF2 gene** *Mol Cell* **7**:509–515 https://doi.org/10.1016/s1097-2765(01)00198-8

28. Martin-Tryon E. L., Harmer S. L 2008) **XAP5 CIRCADIAN TIMEKEEPER coordinates light signals for proper timing of photomorphogenesis and the circadian clock in Arabidopsis** *Plant Cell* **20**:1244–1259 https://doi.org/10.1105/tpc.107.056655

29. Mazzarella R., Pengue G., Yoon J., Jones J., Schlessinger D 1997) **Differential expression of XAP5, a candidate disease gene** *Genomics* **45**:216–219 https://doi.org/10.1006/geno.1997.4912

30. Mitchell D. R 2017) **Evolution of Cilia** *Cold Spring Harb Perspect Biol* **9** https://doi.org/10.1101/cshperspect.a028290

31. Nachury M. V., Mick D. U 2019) **Establishing and regulating the composition of cilia for signal transduction** *Nat Rev Mol Cell Biol* https://doi.org/10.1038/s41580-019-0116-4

32. Nantel F., Monaco L., Foulkes N. S., Masquilier D., LeMeur M., Henriksen K., ..., Sassone-Corsi P. 1996) **Spermiogenesis deficiency and germ-cell apoptosis in CREM-mutant mice** *Nature* **380**:159–162 https://doi.org/10.1038/380159a0

33. Nemajerova A., Kramer D., Siller S. S., Herr C., Shomroni O., Pena T., ..., Lize M. 2016) **TAp73 is a central transcriptional regulator of airway multiciliogenesis** *Genes Dev* **30**:1300–1312 https://doi.org/10.1101/gad.279836.116

34. Oyama Y., Miyata H., Shimada K., Larasati T., Fujihara Y., Ikawa M 2022) **TULP2 deletion mice exhibit abnormal outer dense fiber structure and male infertility** *Reprod Med Biol* **21** https://doi.org/10.1002/rmb2.12467

35. Pertea M., Pertea G. M., Antonescu C. M., Chang T.-C., Mendell J. T., Salzberg S. L 2015) **StringTie enables improved reconstruction of a transcriptome from RNA-seq reads** *Nature Biotechnology* **33**:290–295 https://doi.org/10.1038/nbt.3122

36. Piasecki B. P., Burghoorn J., Swoboda P 2010) **Regulatory Factor X (RFX)-mediated transcriptional rewiring of ciliary genes in animals** *Proc Natl Acad Sci U S A* **107**:12969–12974 https://doi.org/10.1073/pnas.0914241107

37. Qu W., Yuan S., Quan C., Huang Q., Zhou Q., Yap Y., ..., Zhang Z. 2020) **The essential role of intraflagellar transport protein IFT81 in male mice spermiogenesis and fertility** *Am J Physiol Cell Physiol* **318**:C1092–C1106 https://doi.org/10.1152/ajpcell.00450.2019

38. Reinholdt L., Ashley T., Schimenti J., Shima N 2004) **Forward genetic screens for meiotic and mitotic recombination-defective mutants in mice** *Methods Mol Biol* **262**:87–107 https://doi.org/10.1385/1-59259-761-0:087

39. Reiter J. F., Leroux M. R 2017) **Genes and molecular pathways underpinning ciliopathies** *Nat Rev Mol Cell Biol* **18**:533–547 https://doi.org/10.1038/nrm.2017.60

40. Robinson J. T., Thorvaldsdottir H., Turner D., Mesirov J. P 2023) **igv.js: an embeddable JavaScript implementation of the Integrative Genomics Viewer (IGV)** *Bioinformatics* **39** https://doi.org/10.1093/bioinformatics/btac830

41. Romanienko P. J., Camerini-Otero R. D 2000) **The mouse Spo11 gene is required for meiotic chromosome synapsis** *Mol Cell* **6**:975–987 https://doi.org/10.1016/s1097-2765(00)00097-6

42. Santos N., Reiter J. F 2008) **Building it up and taking it down: the regulation of vertebrate ciliogenesis** *Dev Dyn* **237**:1972–1981 https://doi.org/10.1002/dvdy.21540

43. Schartl M., Schories S., Wakamatsu Y., Nagao Y., Hashimoto H., Bertin C., ..., Herpin A. 2018) **Sox5 is involved in germ-cell regulation and sex determination in medaka following co-option of nested transposable elements** *BMC Biol* **16** https://doi.org/10.1186/s12915-018-0485-8

44. Sedlacek Z., Munstermann E., Dhorne-Pollet S., Otto C., Bock D., Schutz G., Poustka A 1999) **Human and mouse XAP-5 and XAP-5-like (X5L) genes: identification of an ancient functional retroposon differentially expressed in testis** *Genomics* **61**:125–132 https://doi.org/10.1006/geno.1999.5931

45. Singla V., Reiter J. F 2006) **The primary cilium as the cell's antenna: signaling at a sensory organelle.** *Science,* **313**:629–633 https://doi.org/10.1126/science.1124534

46. Stubbs J. L., Oishi I., Izpisua Belmonte J. C., Kintner C 2008) **The forkhead protein Foxj1 specifies node-like cilia in Xenopus and zebrafish embryos** *Nat Genet* **40**:1454–1460 https://doi.org/10.1038/ng.267

47. Subramanian A., Tamayo P., Mootha V. K., Mukherjee S., Ebert B. L., Gillette M. A., ..., Mesirov J., P 2005) **Gene set enrichment analysis: A knowledge-based approach for interpreting genome-wide expression profiles** *Proceedings of the National Academy of Sciences* **102**:15545–15550 https://doi.org/10.1073/pnas.0506580102

48. Swoboda P., Adler H. T., Thomas J. H 2000) **The RFX-type transcription factor DAF-19 regulates sensory neuron cilium formation in C. elegans** *Mol Cell* **5**:411–421 https://doi.org/10.1016/s1097-2765(00)80436-0

49. Thomas J., Morle L., Soulavie F., Laurencon A., Sagnol S., Durand B 2010) **Transcriptional control of genes involved in ciliogenesis: a first step in making cilia** *Biol Cell* **102**:499–513 https://doi.org/10.1042/BC20100035

50. Thompson N. A., Ranzani M., van der Weyden L., Iyer V., Offord V., Droop A., ..., Adams D. J. 2021) **Combinatorial CRISPR screen identifies fitness effects of gene paralogues** *Nature Communications* **12** https://doi.org/10.1038/s41467-021-21478-9

51. Vij S., Rink J. C., Ho H. K., Babu D., Eitel M., Narasimhan V., ..., Roy S. 2012) **Evolutionarily ancient association of the FoxJ1 transcription factor with the motile ciliogenic program** *PLoS Genet* **8** https://doi.org/10.1371/journal.pgen.1003019

52. Weidemann M., Schuster-Gossler K., Stauber M., Wrede C., Hegermann J., Ott T., ..., Gossler A. 2016) **CFAP157 is a murine downstream effector of FOXJ1 that is specifically required for flagellum morphogenesis and sperm motility** *Development* **143**:4736–4748 https://doi.org/10.1242/dev.139626

53. Wu Y., Hu X., Li Z., Wang M., Li S., Wang X., ..., Han C. 2016) **Transcription Factor RFX2 Is a Key Regulator of Mouse Spermiogenesis** *Sci Rep* **6** https://doi.org/10.1038/srep20435

54. Yu G., Wang L. G., He Q. Y 2015) **ChIPseeker: an R/Bioconductor package for ChIP peak annotation, comparison and visualization** *Bioinformatics* **31**:2382–2383 https://doi.org/10.1093/bioinformatics/btv145

55. Yu X., Ng C. P., Habacher H., Roy S 2008) **Foxj1 transcription factors are master regulators of the motile ciliogenic program** *Nat Genet* **40**:1445–1453 https://doi.org/10.1038/ng.263

56. Zhang A., Skaar D. A., Li Y., Huang D., Price T. M., Murphy S. K., Jirtle R. L 2011) **Novel retrotransposed imprinted locus identified at human 6p25** *Nucleic Acids Res* **39**:5388–5400 https://doi.org/10.1093/nar/gkr108

57. Zhang D., Xie D., Lin X., Ma L., Chen J., Zhang D., ..., Han C. 2018) **The transcription factor SOX30 is a key regulator of mouse spermiogenesis** *Development* **145** https://doi.org/10.1242/dev.164723

58. Zheng M., Chen X., Cui Y., Li W., Dai H., Yue Q., ..., Zhu H. 2021) **TULP2, a New RNA-Binding Protein, Is Required for Mouse Spermatid Differentiation and Male Fertility** *Front Cell Dev Biol* **9** https://doi.org/10.3389/fcell.2021.623738

59. Zhou H., Grubisic I., Zheng K., He Y., Wang P. J., Kaplan T., Tjian R 2013) **Taf7l cooperates with Trf2 to regulate spermiogenesis** *Proc Natl Acad Sci U S A* **110**:16886–16891 https://doi.org/10.1073/pnas.1317034110

Author information

Weihua Wang*
Institute of Microalgae Synthetic Biology and Green Manufacturing, School of Life Sciences, Jianghan University, Wuhan, China, Hubei Engineering Research Center for Protection and Utilization of Special Biological Resources in the Hanjiang River Basin, School of Life Sciences, Jianghan University, Wuhan, China
ORCID iD: 0009-0007-3965-7375

For correspondence: wangwh2019@163.com
*These authors contributed equally

Junqiao Xing*
Institute of Microalgae Synthetic Biology and Green Manufacturing, School of Life Sciences, Jianghan University, Wuhan, China, Hubei Engineering Research Center for Protection and Utilization of Special Biological Resources in the Hanjiang River Basin, School of Life Sciences, Jianghan University, Wuhan, China

*These authors contributed equally

Xiqi Zhang*
Institute of Microalgae Synthetic Biology and Green Manufacturing, School of Life Sciences, Jianghan University, Wuhan, China

*These authors contributed equally

Hongni Liu
Institute of Microalgae Synthetic Biology and Green Manufacturing, School of Life Sciences, Jianghan University, Wuhan, China, Hubei Engineering Research Center for Protection and Utilization of Special Biological Resources in the Hanjiang River Basin, School of Life Sciences, Jianghan University, Wuhan, China

Xingyu Liu
NO.1 Middle School Affiliated to Central China Normal University, Wuhan, China

Haochen Jiang
Institute of Microalgae Synthetic Biology and Green Manufacturing, School of Life Sciences, Jianghan University, Wuhan, China, Hubei Engineering Research Center for Protection and Utilization of Special Biological Resources in the Hanjiang River Basin, School of Life Sciences, Jianghan University, Wuhan, China
ORCID iD: 0009-0003-4254-6765

Cheng Xu
Institute of Microalgae Synthetic Biology and Green Manufacturing, School of Life Sciences, Jianghan University, Wuhan, China, Hubei Engineering Research Center for Protection and Utilization of Special Biological Resources in the Hanjiang River Basin, School of Life Sciences, Jianghan University, Wuhan, China

Xue Zhao
Institute of Microalgae Synthetic Biology and Green Manufacturing, School of Life Sciences, Jianghan University, Wuhan, China, Hubei Engineering Research Center for Protection and Utilization of Special Biological Resources in the Hanjiang River Basin, School of Life Sciences, Jianghan University, Wuhan, China

Zhangfeng Hu
Institute of Microalgae Synthetic Biology and Green Manufacturing, School of Life Sciences, Jianghan University, Wuhan, China, Hubei Engineering Research Center for Protection and Utilization of Special Biological Resources in the Hanjiang River Basin, School of Life Sciences, Jianghan University, Wuhan, China, Hubei Key Laboratory of Environmental and Health Effects of Persistent Toxic Substances, Jianghan University, Wuhan, China
ORCID iD: 0000-0002-4841-8073

For correspondence: huzhangfenghzf@163.com

Editors

Reviewing Editor
Wei Yan
Washington State University, Pullman, United States of America

Senior Editor
Wei Yan
Washington State University, Pullman, United States of America

Reviewer #1 (Public review):

Summary:

Wang et al. generate XAP5 and XAP5L knockout mice and find that they are male infertile due to spermatogonial/meiotic arrest and reduced sperm motility, respectively. CUT & Tag data were added in this revision in order to support that XAP5 and XAP5L are antagonistic transcription factors of cilliogenesis.

Strengths:

Knockout mouse models provided strong evidence to indicate that XAP5 and XAP5L are critical for spermatogenesis. RNA-seq and CUT & Tag are valuable sources to further explore their molecular mechanisms.

Weaknesses:

The authors claim that XAP5 and XAP5L transcriptionally regulate sperm flagella development; however, expression, physiological role, and molecular evidence do not well support this concept. This reviewer still thinks the physiological roles of XAP5 and XAP5l are different. (i) XAP5 is expressed at spermatogonia within testes while XAP5l is localized at round/elongating spermatids (their expressions are different). (ii) Spermatogenesis was arrested at spermatogonia/early spermatocyte stage in Xap5-KO mice while sperm abnormalities were observed in Xap5l-KO mice (their roles are different). This reviewer still can't get the authors' viewpoint that XAP5 and XAP5l are 'antagonistic relationship' to regulate sperm flagella development. RNA-seq and CUT & Tag data are valuable source; however, this reviewer suggests exploring how XAP5 regulates spermatogonia differentiation and how XAP5l regulates sperm flagella motility.

https://doi.org/10.7554/eLife.94754.2.sa2

Reviewer #2 (Public review):

In this study, Wang et al., report the significance of XAP5L and XAP5 in spermatogenesis which are involved in transcriptional regulation of the ciliary gene in testes. In a previous study, the authors demonstrated that XAP5 is a transcription factor required for flagellar assembly in Chlamydomonas. Continuing from their previous study, the authors examined conserved role of the XAP5 and XAP5L, which are the orthologue pair in mammals.

XAP5 and XAP5L express ubiquitously and testis specifically, respectively, and their absence in testes causes male infertility with defective spermatogenesis. Interestingly, XAP5 deficiency arrest germ cell development at pachytene stage, whereas XAP5L absence causes impaired flagellar formation. RNA-seq analyses demonstrated that XAP5 deficiency suppresses ciliary gene expression including Foxj1 and Rfx family genes in early testis. By contrast, XAP5L deficiency abnormally remains Foxj1 and Rfx genes in mature sperm. From the results, the authors conclude that XAP5 and XAP5L are the antagonistic transcription factor to function at the upstream of Foxj1 and Rfx family genes.

The current version of the manuscript well represents this reviewer's initial concerns and supports author's claim. Key transcription factors for ciliogenesis, Foxj1 and Rfx2, are direct downstream targets for XAP5 and XAP5L and their common motifs well explain their antagonistic function in sperm flagellar development. All the results well demonstrate that ancient transcription factors, XAP5 and XAP5L, are upstream transcription factors to modulate flagellar development in male mammalian germ line.

https://doi.org/10.7554/eLife.94754.2.sa1

Author response:

The following is the authors' response to the original reviews.

> ***Public Reviews:***

> ***Reviewer #1 (Public Review):***
>
> *Summary:*
>
> *Wang et al. generate XAP5 and XAP5L knockout mice and find that they are male infertile due to meiotic arrest and reduced sperm motility, respectively. RNA-Seq was subsequently performed and the authors concluded that XAP5 and XAP5L are antagonistic transcription factors of cilliogenesis (in XAP5-KO P16 testis: 554 genes were unregulated and 1587 genes were downregulated; in XAP5L-KO sperm: 2093 genes were unregulated and 267 genes were downregulated).*

We are grateful for the comprehensive summary.

> *Strengths:*
>
> *Knockout mouse models provided strong evidence to indicate that XAP5 and XAP5L are critical for spermatogenesis and male fertility.*

Thank you for your positive comment.

> *Weaknesses:*
>
> *The key conclusions are not supported by evidence. First, the authors claim that XAP5 and XAP5L transcriptionally regulate sperm flagella development; however, detailed molecular experiments related to transcription regulation are lacking. How do XAP5 and XAP5L regulate their targets? Only RNA-Seq is not enough. Second, the authors declare that XAP5 and XAP5L are antagonistic transcription factors; however, how do XAP5 and XAP5L regulate sperm flagella development antagonistically? Only RNA-Seq is not enough. Third, I am concerned about whether XAP5 really regulates sperm flagella development. XAP5 is specifically expressed in spermatogonia and XAP5-cKO mice are in meiotic arrest, indicating that XAP5 regulates meiosis rather than sperm flagella development.*

Thank you for the critical comments. To strengthen our conclusions, we have included XAP5/XAP5L CUT&Tag data in our revised manuscript. This highly sensitive method has allowed us to identify direct target genes of XAP5 and XAP5L (Table S1, Figure S6). Notably, our results demonstrate that both *FOXJ1* and *RFX2* are occupied by XAP5 (Figure 4G). Additionally, real-time PCR validation confirmed that RFX2 is also associated with XAP5L, even though enriched peaks for the RFX2 gene were not detected in the initial CUT&Tag data (Figure 4G). These findings indicate that XAP5 and XAP5L regulate the expression of FOXJ1 and RFX2 by directly binding to these genes. De novo motif analyses revealed that XAP5 and XAP5L shared a conserved binding sequence (CCCCGCCC/GGGCGGGG) (Figure S6C), and the bound regions of *FOXJ1* and *RFX2* contain this sequence. Further analysis shows that many XAP5L target genes are also targets of XAP5 (Figure S6G), despite the limited number of identified XAP5L target genes. This differential binding and regulation of shared target genes underscore the antagonistic relationship between XAP5 and XAP5L. Collectively, these findings provide additional support for the idea that XAP5 and XAP5L function as antagonistic transcription factors, acting upstream of transcription factor families, including FOXJ1 and RFX factors, to coordinate ciliogenesis during spermatogenesis.

While we agree that XAP5 primarily regulates meiosis during spermatogenesis, our data also indicate that many cilia-related genes, including key transcription regulators of spermiogenesis such as RFX2 and SOX30, are downregulated in XAP5-cKO mice and are bound by XAP5 (Figure 4, Figures S4 and S6). It is important to note that genes coding for flagella components are expressed sequentially and in a germ cell-specific manner during

development. When we refer to "regulating sperm flagella development", we mean the spatiotemporal regulation. We have revised the manuscript to clarify this point.

> ***Reviewer #2 (Public Review):***
>
> *In this study, Wang et al., report the significance of XAP5L and XAP5 in spermatogenesis, involved in transcriptional regulation of the ciliary gene in testes. In previous studies, the authors demonstrate that XAP5 is a transcription factor required for flagellar assembly in Chlamydomonas. Continuing from their previous study, the authors examine the conserved role of the XAP5 and XAP5L, which are the orthologue pair in mammals.*
>
> *XAP5 and XAP5L express ubiquitously and testis specifically, respectively, and their absence in the testes causes male infertility with defective spermatogenesis. Interestingly, XAP5 deficiency arrests germ cell development at the pachytene stage, whereas XAP5L absence causes impaired flagellar formation. RNA-seq analyses demonstrated that XAP5 deficiency suppresses ciliary gene expression including Foxj1 and Rfx family genes in early testis. By contrast, XAP5L deficiency abnormally remains Foxj1 and Rfx genes in mature sperm. From the results, the authors conclude that XAP5 and XAP5L are the antagonistic transcription factors that function upstream of Foxj1 and Rfx family genes.*
>
> *This reviewer thinks the overall experiments are performed well and that the manuscript is clear. However, the current results do not directly support the authors' conclusion. For example, the transcriptional function of XAP5 and XAP5L requires more evidence. In addition, this reviewer wonders about the conserved XAP5 function of ciliary/flagellar gene transcription in mammals - the gene is ubiquitously expressed despite its functional importance in flagellar assembly in Chlamydomonas. Thus, this reviewer thinks authors are required to show more direct evidence to clearly support their conclusion with more descriptions of its role in ciliary/flagellar assembly.*

Thank you for your thoughtful review of our work. We appreciate your positive feedback on the overall quality of the experiments and the clarity of the manuscript. In response to your concerns, we have included new experimental data and made revisions to the manuscript (lines 193-217) to better support our conclusions, particularly regarding the transcriptional function of XAP5 and XAP5L. Additionally, we have expanded on the role of XAP5 in ciliary and flagellar assembly to provide more direct evidence for its functional importance. Thank you for your insights.

> ***Recommendations for the authors:***
>
> ***Reviewer #1 (Recommendations For The Authors):***
>
> *The title (Control of ciliary transcriptional programs during spermatogenesis by antagonistic transcription factors) is not specific and does tend to exaggerate.*

Thank you for the comment, and we appreciate the opportunity to clarify the appropriateness of the title. Our paper extensively investigates the transcriptional regulation of ciliary genes during spermatogenesis. It demonstrates that XAP5/XAP5L are key transcription factors involved in this process. The title reflects our primary focus on the transcriptional programs that govern ciliary gene expression. Moreover, our paper shows that XAP5 positively regulates the expression of ciliary genes, particularly during the early stages of spermatogenesis, while XAP5L negatively regulates these genes. This antagonistic relationship is a crucial aspect of the study and is effectively conveyed in the title. In addition, our revised paper provides detailed insights into how XAP5/XAP5L control ciliary gene expression during spermatogenesis.

> *Figure 4C: FOXJ1 and RFX2 are absent in sperm from WT mice. Are you sure? They are highly expressed in WT testes.*

Thank you for your careful review. While FOXJ1 and RFX2 are indeed highly expressed in the testes of wild-type (WT) mice, our data show that they are not detectable in mature sperm. This observation is consistent with published single-cell RNA-seq data(Jung et al., 2019), which indicate that FOXJ1 and RFX2 are primarily expressed in spermatocytes but not in spermatids (Figure S7). This expression pattern aligns with that that of IFT-particle proteins, which are essential for the formation but not the maintenance of mammalian sperm flagella(San Agustin, Pazour, & Witman, 2015).

> *XAP5 is specifically expressed in spermatogonia and XAP5-cKO mice are in meiotic arrest, indicating that XAP5 regulates meiosis rather than sperm flagella development.*

We appreciate your insightful comments. As mentioned above, we agree that XAP5 primarily regulates meiosis during spermatogenesis. When we mentioned "regulating sperm flagella development," we were referring to the spatiotemporal regulation of these processes. We have revised the manuscript to clarify this distinction. Thank you for your understanding.

> *The title of Figure 2 (XAP5L is required for normal sperm formation) is not accurate because the progress of spermatogenesis and sperm count is normal in XAP5L-KO mice (only sperm motility is reduced).*

We apologize for any confusion caused by the previous figure. It did not accurately convey the changes in sperm count. In the revised Figure 2B, we clearly demonstrate that the sperm count in XAP5L-KO mice is indeed lower than that in WT mice. This revision aims to provide a more accurate representation of the effects of XAP5L deficiency on spermatogenesis. Thank you for bringing this to our attention.

> ***Reviewer #2 (Recommendations For The Authors):***
>
> *(1) Although XAP5 and XAP5L deficiency alters the transcription of Foxj1 and Rfx family genes, which are the essential transcription factors for the ciliogenesis, current data do not directly support that XAP5 and XAP5L are the upstream transcription factors. The authors need to show more direct evidence such as CHIP-Seq data.*

Thank you for your valuable feedback! In this revised manuscript, we have included data identifying candidate direct targets of XAP5 and XAP5L using the highly sensitive CUT&Tag method (Kaya-Okur et al., 2019). Our results show that XAP5 occupies both FOXJ1 and RFX2 (Figure 4G). Furthermore, real-time PCR validation of the CUT&Tag experiments confirmed that RFX2 is also occupied by XAP5L (Figure 4G), despite the initial CUT&Tag data not revealing enriched peaks for the RFX2 gene (Table S1). Unfortunately, the limited number of enriched peaks identified for XAP5L (Table S1) suggests that the XAP5L antibody used in the CUT&Tag experiment might have suboptimal performance, which prevented us from detecting occupancy on the FOXJ1 promoter. Nevertheless, these additional data provide strong evidence that XAP5 and XAP5L function as upstream transcription factors for FOXJ1 and RFX family genes, supporting their essential roles in ciliogenesis.

> *(2) Shared transcripts that are altered by the absence of either XAP5 or XAP5L do not clearly support they are antagonistic transcription factors.*

Thank you for your insightful comment. In our revised manuscript, we performed CUT&Tag analysis to identify target genes of XAP5 and XAP5L. Motif enrichment analysis revealed

conserved binding sequences for both factors (Figures S6C), indicating a subset of shared downstream genes between XAP5 and XAP5L. Among the downregulated genes in XAP5 cKO germ cells, 891 genes were bound by XAP5 (Figure S6D). Although the number of enriched peaks identified for XAP5L was limited, 75 of the upregulated genes in XAP5L KO sperm were bound by XAP5L (Figure S6E). Importantly, of these 75 XAP5L target genes, approximately 30% (22 genes) were also identified as targets of XAP5 (Figure S6G), further support the idea that XAP5 and XAP5L function as antagonistic transcription factors.

> *(3) XAP5 seems to be an ancient transcription factor for cilia and flagellar assembly. However, XAP5 expresses ubiquitously in mice. How can this discrepancy be explained? Is it also required for primary cilia assembly? Are their expression also directly linked to ciliogenesis in other types of cells?*

Thank you for the thoughtful questions. The ubiquitous expression of XAP5 in mice can be understood in light of its role as an ancient transcription factor for cilia and flagellar assembly. Given that cilia are present on nearly every cell type in the mammalian body (O'Connor et al., 2013), this broad expression pattern makes sense. In fact, XAP5 serves not only as a master regulator of ciliogenesis but also as a critical regulator of various developmental processes (Kim et al., 2018; Lee et al., 2020; Xie et al., 2023).

Our current unpublished work demonstrates that XAP5 is essential for primary cilia assembly in different cell lines. The loss of XAP5 protein results in abnormal ciliogenesis, further supporting its vital role in ciliary formation across different cell types.

We believe that the widespread expression of XAP5 reflects its fundamental importance in multiple cellular processes, including ciliogenesis, development, and potentially other cellular functions yet to be discovered.

> *(4) XAP5L causes impairs flagellar assembly. Have the authors observed any other physiological defects in the absence of XAP5L in mouse models? Such as hydrocephalus and/or tracheal defects?*

Thank you for the questions. We have carefully examined *XAP5L* KO mice for other physiological defects. To date, we have not observed any additional physiological abnormalities. Specifically, we assessed the condition of tracheal cilia in *XAP5L* KO mice and found no significant differences compared to wild-type (WT) mice, as illustrated in Author response image 1 below.

Author response image 1.

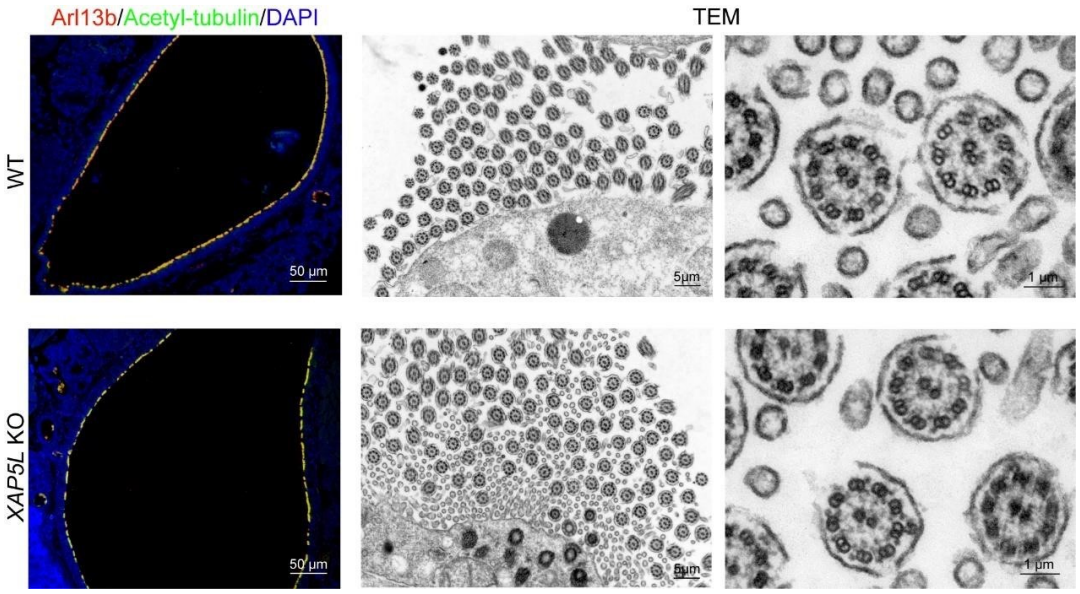

References

Jung, M., Wells, D., Rusch, J., Ahmad, S., Marchini, J., Myers, S. R., & Conrad, D. F. (2019). Unified single-cell analysis of testis gene regulation and pathology in five mouse strains. *Elife, 8*. doi:10.7554/eLife.43966

Kaya-Okur, H. S., Wu, S. J., Codomo, C. A., Pledger, E. S., Bryson, T. D., Henikoff, J. G., . . . Henikoff, S. (2019). CUT&Tag for efficient epigenomic profiling of small samples and single cells. *Nat Commun, 10*(1), 1930. doi:10.1038/s41467-019-09982-5

Kim, Y., Hur, S. W., Jeong, B. C., Oh, S. H., Hwang, Y. C., Kim, S. H., & Koh, J. T. (2018). The Fam50a positively regulates ameloblast differentiation via interacting with Runx2. *J Cell Physiol, 233*(2), 1512-1522. doi:10.1002/jcp.26038

Lee, Y.-R., Khan, K., Armfield-Uhas, K., Srikanth, S., Thompson, N. A., Pardo, M., . . . Schwartz, C. E. (2020). Mutations in FAM50A suggest that Armfield XLID syndrome is a spliceosomopathy. *Nature Communications, 11*(1). doi:10.1038/s41467-020-17452-6

O'Connor, A. K., Malarkey, E. B., Berbari, N. F., Croyle, M. J., Haycraft, C. J., Bell, P. D., . . . Yoder, B. K. (2013). An inducible CiliaGFP mouse model for in vivo visualization and analysis of cilia in live tissue. *Cilia, 2*(1), 8. doi:10.1186/2046-2530-2-8

San Agustin, J. T., Pazour, G. J., & Witman, G. B. (2015). Intraflagellar transport is essential for mammalian spermiogenesis but is absent in mature sperm. *Mol Biol Cell, 26*(24), 4358-4372. doi:10.1091/mbc.E15-08-0578

Xie, X., Li, L., Tao, S., Chen, M., Fei, L., Yang, Q., . . . Chen, L. (2023). Proto-Oncogene FAM50A Can Regulate the Immune Microenvironment and Development of Hepatocellular Carcinoma In Vitro and In Vivo. *Int J Mol Sci, 24*(4). doi:10.3390/ijms24043217

https://doi.org/10.7554/eLife.94754.2.sa0